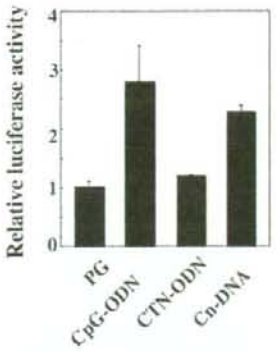

FIGURE 7. NF-κB activation via TLR9 by cryptococcal DNA. HEK293T cells transfected with the TLR9 gene or control vector were treated with CpG1826 (300 nM), PG (1 μg/ml), or Cap67 DNA (250 μg/ml) for 6 h. The luciferase activity in each sample was determined as described in *Materials and Methods*. Data are expressed as relative values to those of control vector and presented are mean ± SD of triplicate cultures. CNT-ODN, control ODN of CpG1826.

IL-12p40 by BM-DCs from both mice, which may raise a possibility that capsular polysaccharides affect the activation of BM-DCs caused by cryptococcal DNA. We tested the effect of the culture supernatants of YC-11 on the IL-12p40 production by BM-DCs. As shown in Fig. 4*d*, the production of this cytokine caused by cryptococcal DNA was strongly inhibited by the YC-11 culture supernatants in a dose-dependent fashion, whereas such inhibition was not found when BM-DCs were stimulated with LPS. In addition, we compared the clinical course of infection with Cap67 in lungs between TLR9$^{-/-}$ and WT mice. As shown in Fig. 4*e*, the number of live colonies in lungs was significantly higher in the former mice than in the latter ones 2 wk after infection, although dissemination of yeast cells to brains was not detected in both groups (data not shown).

In additional experiments, we tested how Cap67 DNA-induced activation of BM-DCs was affected in mice genetically lacking MyD88, a downstream signaling molecule of TLR9 and TLR4, or TRIF, that of TLR4, but not of TLR9 (37). BM-DCs from MyD88$^{-/-}$ mice failed to produce IL-12p40 induced by Cap67 DNA and LPS, but not by OX-CA (Fig. 5*a*). In contrast, LPS, but not Cap67 DNA and OX-CA, inhibited such production by BM-DCs from TRIF$^{-/-}$ mice (Fig. 5*a*). Similarly, CD40 expression induced by Cap67 DNA and CpG1826 was completely abrogated in MyD88$^{-/-}$ mice, whereas such expression was not affected in the case of OX-CA stimulation (Fig. 5*b*). Similar results were obtained for the synthesis of IL-12p40, when BM-DCs were stimulated with whole yeast cells (data not shown). These results indicate that TLR9 and its downstream signaling molecule are essential for Cap67 DNA-induced activation of BM-DCs.

Methylation of the CpG motif results in the loss of its capability to activate DCs via a TLR9-dependent signaling pathway (16, 24). Therefore, we tested the effect of methylation on cytokine synthesis by Cap67 DNA-stimulated BM-DCs. As shown in Fig. 6, BM-DCs stimulated by CpG1826 and Cap67 DNA pretreated with methylase did not synthesize IL-12p40. These results were consistent with the notion that Cn DNA activates BM-DCs by interacting with TLR9.

Cn DNA activates the signaling pathway via TLR9

CpG-ODN triggers the signaling pathway via TLR9, which results in the activation of NF-κB (37). In the next step, we tested the effect of Cn DNA on NF-κB. For this purpose, we performed a luciferase reporter assay using HEK293T cells transfected with the gene for TLR9 and luciferase gene linked to the promoter sequence containing an NF-κB binding site. As shown in Fig. 7, both Cap67 DNA and CpG1826 induced luciferase activity in TLR9-expressing HEK293T cells, whereas PG and control ODN of CpG1826 did not show such activity. These results indicate that Cn DNA triggered the signaling pathway for activation of NF-κB by directly interacting with TLR9.

Colocalization of Cn DNA with CpG-ODN in BM-DCs

In DCs and macrophages, CpG-ODN is internalized into early endosomes, followed by subsequent transportation to a lysosomal compartment and direct interaction with TLR9, which is redistributed from the endoplasmic reticulum (19, 20). Using confocal microscopic analysis, we compared the intracellular trafficking of Cap67 DNA and CpG1826 to further define the relationship of both agents during the activation of BM-DCs. As shown in Fig. 8*a*, Cap67 DNA and CpG1826 were mostly colocalized in the intracellular area of BM-DCs at 5, 30, 60, and 90 min after incubation. Thus, the intracellular trafficking of Cn DNA in BM-DCs is similar to that of CpG1826, suggesting the interaction of the fungal DNA with TLR9. In the next step, we analyzed the distribution of TLR9 in these cells after incubation with Cap67 DNA and CpG1826. Isotype-matched irrelevant Ab did not show positive staining in resting and Cap67 DNA-stimulated BM-DCs (data not shown). TLR9 was detected in the intracellular area of resting BM-DCs and redistributed in part to the area where these nucleic acids were localized after stimulation, and similar results were obtained using RAW264.1 cells, a macrophage lineage cell line (Fig. 8*b*). These results indicate that Cn DNA interacts with TLR9 in the endosomal pathway similar to CpG1826.

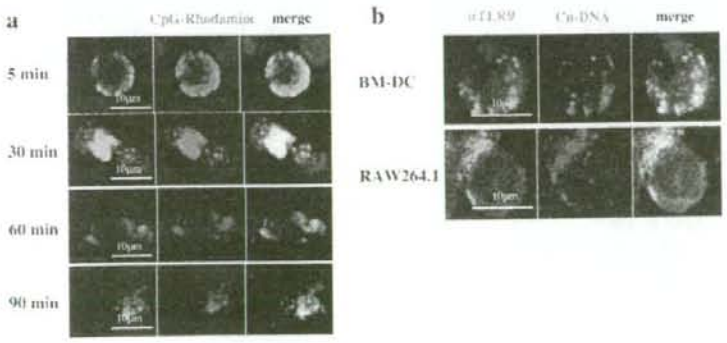

FIGURE 8. Trafficking of cryptococcal DNA in BM-DCs and colocalization with TLR9. *a*, BM-DCs were simultaneously incubated with 10 μg/ml Alexa Fluor 647-conjugated Cap67 DNA (green) and 3 μM CpG-rhodamine (red) for the indicated time periods. *b*, BM-DCs or RAW264.1 cells were incubated with 10 μg/ml Alexa Fluor 647-Cap67 DNA (red) for 30 min. After fixation, TLR9 was stained intracellularly by direct immunofluorescence with FITC-conjugated anti-TLR9 Ab (green). Cells were analyzed using a confocal microscope. Data are representative of three to four independent experiments.

Discussion

In the present study, we hypothesized that DNA from Cn can activate BM-DCs based on the finding that lysates of this fungal microorganism showed such activity, which was significantly reduced after DNase treatment. In agreement with this hypothesis, cryptococcal DNA induced the release of IL-12p40 and expression of CD40 by BM-DCs. Such activity was not mediated by contaminated LPS or β-glucan due to the following reasons: 1) the activity was abrogated by DNase treatment, 2) polymixin B did not affect the activity, and 3) the level of activity was similar in BM-DCs from control mice, C3H/HeJ, and TLR4$^{-/-}$ mice (data not shown) and from dectin-1$^{-/-}$ mice lacking a specific receptor for β-glucan. In addition, activation of BM-DCs did not involve capsular polysaccharides because DNA from an acapsular strain of Cn was highly active. In earlier studies (24, 25), similar to our findings, DNA from two yeast-form fungi, *S. pompe* and *P. brasiliensis*, also induced the B cell proliferation and the development of Th1 immune responses and host protection, respectively, although the precise mechanism was not investigated. Thus, Cn seems to possess immunostimulatory DNA that promotes Th1-mediated host responses against this infection.

In previous studies (12, 13), MyD88, which acts as an adaptor molecule in signaling via TLRs (37), was reported to play an important role in host defense against cryptococcal infection. These findings suggested the possible involvement of certain TLRs. However, involvement of TLR2 and TLR4 in the host defense responses against this infection remains to be substantiated (12–14). Recent studies have identified the involvement of TLRs in the recognition of nucleic acids; including TLR3 for dsRNA, TLR7/8 for ssRNA, and TLR9 for unmethylated CpG motif-containing DNA (18, 38–40). Thus, we addressed the possible contribution of TLR9 to the mechanism underlying cryptococcal DNA-induced BM-DC activation, although it was unclear whether Cn possess such motifs in its DNA structure. CpG-ODN is internalized via an endocytic pathway and trafficked into late endosomal compartments, followed by direct interaction with TLR9 (19, 20). In this process, acidification of the endosomal compartments is required, which is blocked by chloroquine and bafilomycin A (35). As expected, cytokine synthesis and expression of costimulatory cell surface molecules induced by cryptococcal DNA was strongly suppressed by these compounds, as they acted on CpG-ODN-induced responses. Furthermore, inhibitory ODN that block the signaling triggered by CpG-ODN in a specific manner (36) suppressed the activation of BM-DCs caused by cryptococcal DNA as well as CpG-ODN. Theses results suggest that Cn DNA was recognized by TLR9 for its capacity to activate BM-DCs, similar to the case of CpG-ODN.

In agreement with this possibility, the effects of cryptococcal DNA required the presence of TLR9, as shown in the present results, in which the production of IL-12p40 and expression of CD40 by BM-DCs stimulated with cryptococcal DNA were cancelled in TLR9$^{-/-}$ mice, similar to the results seen upon the use of CpG-ODN. The TLR9 signaling is dependent on an adaptor molecule, MyD88, but not on TRIF, the latter of which mediates the signals triggered by TLR3 and TLR4 (37). This notion is consistent with our findings of failure of activation of BM-DCs from MyD88$^{-/-}$ mice, but not from TRIF$^{-/-}$ mice, when stimulated by cryptococcal DNA. These results suggest that cryptococcal DNA triggers TLR9 and delivers the activation signals with MyD88. In agreement with this scenario, methylation of cryptococcal DNA led to a reduction in its ability to induce cytokine synthesis by BM-DCs, a treatment known to diminish the activity of CpG-ODN via interaction with TLR9 (16, 24). In addition, using a NF-κB reporter assay, cryptococcal DNA triggered the activation signals in HEK293 transfected with the TLR9 gene. Thus, to our best knowledge, fungal DNA was first found to promote the activation of BM-DCs by triggering the TLR9-dependent and MyD88-mediated signaling pathway. In this study, methylation of cryptococcal DNA did not completely abrogate its ability to stimulate cytokine synthesis by BM-DCs, in contrast to the effect of this treatment on CpG-ODN. Although a possibility that cryptococcal DNA was not completely methylated is not excluded, these data suggest a TLR9-mediated, but CpG-independent activation mechanism for cryptococcal DNA, which may be consistent with the recent observations that TLR9 recognizes DNA not only by the CpG motif but also by different nucleic acid sequences (41).

In the present study, BM-DCs were stimulated by adding cryptococcal DNA to the cell cultures, suggesting that the DNA was internalized through the cell membranes and moved into the endosomal pathway as described previously for CpG-ODN (19, 20). This possibility was confirmed using confocal microscopy performed by comparing the intracellular trafficking of fluorescence-labeled cryptococcal DNA and CpG-ODN. The results showed colocalization of these two nucleic acids throughout the course of incubation. Thus, the intracellular trafficking of cryptococcal ODN to the endosomal pathway is similar to that of the CpG-ODN. Latz et al. (19) demonstrated the redistribution of TLR9 toward the sites of CpG-ODN accumulation. Compatible with this observation, in the present study, redistribution of TLR9 to the sites of cryptococcal DNA accumulation was noted in BM-DCs. These results add further support to our conclusion that cryptococcal DNA activated BM-DCs for cytokine synthesis and expression of costimulatory cell surface molecules by triggering the TLR9 signaling pathway, although we could not confirm that cryptococcal DNA directly binds TLR9.

Based on our findings, we propose here a novel mechanism for recognition of fungal pathogen by the host immune system: the DCs sense Cn DNA in a TLR9-dependent fashion. Cn infects lung tissues and multiplies in alveolar spaces. It has recently been proposed that this fungal pathogen grows inside the endosomes of macrophages based on its escape mechanism against killing effector molecules (1). Macrophages acquire the capacity to kill the fungus after their activation by IFN-γ secreted from Th1 cells (5). Therefore, it is unlikely that the DNA is released from Cn outside the macrophages and DCs, but rather generated from the killed yeast cells in the endosomal compartment, which could be moved into the TLR9-triggered signaling pathway for the initiation of host protective immune responses. Consistent with this notion, activation of BM-DCs by whole cryptococcal cells was significantly, although not completely, reduced in TLR9$^{-/-}$ mice, and these mice were more susceptible to pulmonary infection with Cn than WT control mice, as shown by the increased live colonies in lungs, when Cap67, an acapsular strain, was used. In this regard, it was recently demonstrated that DCs could incorporate and kill this fungal microorganism (42, 43). In our data, the culture supernatants of YC-11, a highly encapsulated Cn, containing much capsular polysaccharides suppressed the production of IL-12p40 by cryptococcal DNA and, in addition, BM-DCs failed to produce IL-12p40 upon stimulation with whole yeast cells of YC-11 in contrast to Cap67 (Fig. 4, *c* and *d*), although DNA from the former strain was as potent as the latter ones (Fig. 1*e*). These observations raise a possibility that capsular polysaccharides interfere with the BM-DC production of IL-12p40 in response to cryptococcal DNA, which may limit the significance of our findings. However, Cn is known to have no capsule or a thin capsule when infected via the airborne route, which may provide a benefit for them to reach the alveolar space (44). This notion suggests that DCs may encounter acapsular

or thinly capsulated Cn and may be activated by DNA released from engulfed yeast cells under little influence of capsular polysaccharides at the early stage of infection. Further investigations are necessary to address this important issue.

Thus, the present findings enhance our understanding of the pathogenic mechanism of intractable cryptococcal infection in immunocompromised patients and help in the design of novel immunotherapies to combat such clinically difficult infection.

Disclosures

The authors have no financial conflict of interest.

References

1. Feldmesser, M., S. Tucker, and A. Casadevall. 2001. Intracellular parasitism of macrophages by *Cryptococcus neoformans*. *Trends Microbiol.* 9: 273–278.
2. Lim, T. S., and J. W. Murphy. 1980. Transfer of immunity to cryptococcosis by T-enriched splenic lymphocytes from *Cryptococcus neoformans*-sensitized mice. *Infect. Immun.* 30: 5–11.
3. Mody, C. H., M. F. Lipscomb, N. E. Street, and G. B. Toews. 1990. Depletion of $CD4^+L3T4^+$ lymphocytes in vivo impairs murine host defense to *Cryptococcus neoformans*. *J. Immunol.* 144: 1472–1477.
4. Hill, J. O., and A. G. Harmsen. 1991. Intrapulmonary growth and dissemination of an avirulent strain of *Cryptococcus neoformans* in mice depleted of $CD4^+$ or $CD8^+$ T cells. *J. Exp. Med.* 173: 755–758.
5. Koguchi, Y., and K. Kawakami. 2002. Cryptococcal infection and Th1-Th2 cytokine balance. *Int. Rev. Immunol.* 21: 423–438.
6. Mansour, M. K., E. Latz, and S. M. Levitz. 2006. *Cryptococcus neoformans* glycoantigens are captured by multiple lectin receptors and presented by dendritic cells. *J. Immunol.* 176: 3053–3061.
7. Lipscomb, M. F., T. Alvarellos, G. B. Toews, R. Tompkins, Z. Evans, G. Koo, and V. Kumar. 1987. Role of natural killer cells in resistance to *Cryptococcus neoformans* infections in mice. *Am. J. Pathol.* 128: 354–361.
8. Kawakami, K., Y. Kinjo, K. Uezu, S. Yara, K. Miyagi, Y. Koguchi, T. Nakayama, M. Taniguchi, and A. Saito. 2001. Monocyte chemoattractant protein-1-dependent increase of Vα14 NKT cells in lungs and their roles in Th1 response and host defense in cryptococcal infection. *J. Immunol.* 167: 6525–6532.
9. Uezu, K., K. Kawakami, K. Miyagi, Y. Kinjo, T. Kinjo, H. Ishikawa, and A. Saito. 2004. Accumulation of γδ T cells in the lungs and their regulatory roles in Th1 response and host defense against pulmonary infection with *Cryptococcus neoformans*. *J. Immunol.* 172: 7629–7634.
10. Mednick, A. J., M. Feldmesser, J. Rivera, and A. Casadevall. 2003. Neutropenia alters lung cytokine production in mice and reduces their susceptibility to pulmonary cryptococcosis. *Eur. J. Immunol.* 33: 1744–1753.
11. Takeda, K., T. Kaisho, and S. Akira. 2003. Toll-like receptors. *Annu. Rev. Immunol.* 21: 335–376.
12. Yauch, L. E., M. K. Mansour, S. Shoham, J. B. Rottman, and S. M. Levitz. 2004. Involvement of CD14, Toll-like receptors 2 and 4, and MyD88 in the host response to the fungal pathogen *Cryptococcus neoformans* in vivo. *Infect. Immun.* 72: 5373–5382.
13. Biondo, C., A. Midiri, L. Messina, F. Tomasello, G. Garufi, M. R. Catania, M. Bombaci, C. Beninati, G. Teti, and G. Mancuso. 2005. MyD88 and TLR2, but not TLR4, are required for host defense against *Cryptococcus neoformans*. *Eur. J. Immunol.* 35: 870–878.
14. Nakamura, K., K. Miyagi, Y. Koguchi, Y. Kinjo, K. Uezu, T. Kinjo, M. Akamine, J. Fujita, I. Kawamura, M. Mitsuyama, et al. 2006. Limited contribution of Toll-like receptor 2 and 4 to the host response to a fungal infectious pathogen, *Cryptococcus neoformans*. *FEMS Immunol. Med. Microbiol.* 47: 148–154.
15. Shoham, S., C. Huang, J. M. Chen, D. T. Golenbock, and S. M. Levitz. 2001. Toll-like receptor 4 mediates intracellular signaling without TNF-α release in response to *Cryptococcus neoformans* polysaccharide capsule. *J. Immunol.* 166: 4620–4626.
16. Krieg, A. M., A. K. Yi, S. Matson, T. J. Waldschmidt, G. A. Bishop, R. Teasdale, G. A. Koretzky, and D. M. Klinman. 1995. CpG motifs in bacterial DNA trigger direct B-cell activation. *Nature* 374: 546–549.
17. Krieg, A. M. 2002. CpG motifs in bacterial DNA and their immune effects. *Annu. Rev. Immunol.* 20: 709–760.
18. Hemmi, H., O. Takeuchi, T. Kawai, T. Kaisho, S. Sato, H. Sanjo, M. Matsumoto, K. Hoshino, H. Wagner, K. Takeda, and S. Akira. 2000. A Toll-like receptor recognizes bacterial DNA. *Nature* 408: 740–745.
19. Latz, E., A. Schoenemeyer, A. Visintin, K. A. Fitzgerald, B. G. Monks, C. F. Knetter, E. Lien, N. J. Nilsen, T. Espevik, and D. T. Golenbock. 2004. TLR9 signals after translocating from the ER to CpG DNA in the lysosome. *Nat. Immunol.* 5: 190–198.
20. Honda, K., Y. Ohba, H. Yanai, H. Negishi, T. Mizutani, A. Takaoka, C. Taya, and T. Taniguchi. 2005. Spatiotemporal regulation of MyD88-IRF-7 signalling for robust type-I interferon induction. *Nature* 434: 1035–1040.
21. Kawai, T., S. Sato, K. J. Ishii, C. Coban, H. Hemmi, M. Yamamoto, K. Terai, M. Matsuda, J. Inoue, S. Uematsu, et al. 2004. Interferon-α induction through Toll-like receptors involves a direct interaction of IRF7 with MyD88 and TRAF6. *Nat. Immunol.* 5: 1061–1068.
22. Brown, W. C., D. M. Estes, S. E. Chantler, K. A. Kegerreis, and C. E. Suarez. 1998. DNA and a CpG oligonucleotide derived from *Babesia bovis* are mitogenic for bovine B cells. *Infect. Immun.* 66: 5423–5432.
23. Shoda, L. K., K. A. Kegerreis, C. E. Suarez, I. Roditi, R. S. Corral, G. M. Bertot, J. Norimine, and W. C. Brown. 2001. DNA from protozoan parasites *Babesia bovis*, *Trypanosoma cruzi*, and *T. brucei* is mitogenic for B lymphocytes and stimulates macrophage expression of interleukin-12, tumor necrosis factor α, and nitric oxide. *Infect. Immun.* 69: 2162–2171.
24. Sun, S., C. Beard, R. Jaenisch, P. Jones, and J. Sprent. 1997. Mitogenicity of DNA from different organisms for murine B cells. *J. Immunol.* 159: 3119–3125.
25. Souza, M. C., M. Correa, S. R. Almeida, J. D. Lopes, and Z. P. Camargo. 2001. Immunostimulatory DNA from *Paracoccidioides brasiliensis* acts as T-helper 1 promoter in susceptible mice. *Scand. J. Immunol.* 54: 348–356.
26. Yamamoto, M., S. Sato, H. Hemmi, K. Hoshino, T. Kaisho, H. Sanjo, O. Takeuchi, M. Sugiyama, M. Okabe, K. Takeda, and S. Akira. 2003. Role of adaptor TRIF in the MyD88-independent Toll-like receptor signaling pathway. *Science* 301: 640–643.
27. Adachi, O., T. Kawai, K. Takeda, M. Matsumoto, H. Tsutsui, M. Sakagami, K. Nakanishi, and S. Akira. 1998. Targeted disruption of the MyD88 gene results in loss of IL-1- and IL-18-mediated function. *Immunity* 9: 143–150.
28. Saijo, S., N. Fujikado, T. Furuta, H. Kotaki, K. Seki, K. Sudo, S. Akira, Y. Adachi, N. Ohno, T. Kinjo, et al. 2007. Dectin-1 plays an important role in the host defense mechanism against pathogenic fungus *Pneumocystis carinii* under immuno-compromised conditions. *Nat. Immunol.* 8: 39–46.
29. Yasuoka, A., S. Kohno, H. Yamada, M. Kaku, and H. Koga. 1994. Influence of molecular sizes of *Cryptococcus neoformans* capsular polysaccharide on phagocytosis. *Microbiol. Immunol.* 38: 851–856.
30. Ishibashi, K., N. Miura, Y. Adachi, N. Ogura, H. Tamura, S. Tanaka, and N. Ohno. 2004. DNA array analysis of altered gene expression in human leukocytes stimulated with soluble and particulate forms of *Candida* cell wall β-glucan. *Int. Immunopharmacol.* 4: 387–401.
31. Lutz, M. B., N. Kukutsch, A. L. Ogilvie, S. Rossner, F. Koch, N. Romani, and G. Schuler. 1999. An advanced culture method for generating large quantities of highly pure dendritic cells from mouse bone marrow. *J. Immunol. Methods* 223: 77–92.
32. Chuang, T. H., J. Lee, L. Kline, J. C. Mathison, and R. J. Ulevitch. 2002. Toll-like receptor 9 mediates CpG-DNA signaling. *J. Leukocyte Biol.* 71: 538–544.
33. Monari, C., F. Bistoni, and A. Vecchiarelli. 2006. Glucuronoxylomannan exhibits potent immunosuppressive properties. *FEMS Yeast Res.* 6: 537–542.
34. Gantner, B. N., R. M. Simmons, S. J. Canavera, S. Akira, and D. M. Underhill. 2003. Collaborative induction of inflammatory responses by dectin-1 and Toll-like receptor 2. *J. Exp. Med.* 197: 1107–1117.
35. Hacker, H., H. Mischak, T. Miethke, S. Liptay, R. Schmid, T. Sparwasser, K. Heeg, G. B. Lipford, and H. Wagner. 1998. CpG-DNA-specific activation of antigen-presenting cells requires stress kinase activity and is preceded by non-specific endocytosis and endosomal maturation. *EMBO J.* 17: 6230–6240.
36. Stunz, L. L., P. Lenert, D. Peckham, A. K. Yi, S. Haxhinasto, M. Chang, A. M. Krieg, and R. F. Ashman. 2002. Inhibitory oligonucleotides specifically block effects of stimulatory CpG oligonucleotides in B cells. *Eur. J. Immunol.* 32: 1212–1222.
37. Akira, S., and K. Takeda. 2004. Toll-like receptor signalling. *Nat. Rev. Immunol.* 4: 499–511.
38. Alexopoulou, L., A. C. Holt, R. Medzhitov, and R. A. Flavell. 2001. Recognition of double-stranded RNA and activation of NF-κB by Toll-like receptor 3. *Nature* 413: 732–738.
39. Hemmi, H., T. Kaisho, O. Takeuchi, S. Sato, H. Sanjo, K. Hoshino, T. Horiuchi, H. Tomizawa, K. Takeda, and S. Akira. 2002. Small anti-viral compounds activate immune cells via the TLR7 MyD88-dependent signaling pathway. *Nat. Immunol.* 3: 196–200.
40. Vollmer, J., S. Tluk, C. Schmitz, S. Hamm, M. Jurk, A. Forsbach, S. Akira, K. M. Kelly, W. H. Reeves, S. Bauer, and A. M. Krieg. 2005. Immune stimulation mediated by autoantigen binding sites within small nuclear RNAs involves Toll-like receptors 7 and 8. *J. Exp. Med.* 202: 1575–1585.
41. Vollmer, J., R. D. Weeratna, M. Jurk, U. Samulowitz, M. J. McCluskie, P. Payette, H. L. Davis, C. Schetter, and A. M. Krieg. 2004. Oligodeoxynucleotides lacking CpG dinucleotides mediate Toll-like receptor 9 dependent T helper type 2 biased immune stimulation. *Immunology* 113: 212–223.
42. Syme, R. M., J. C. Spurrell, E. K. Amankwah, F. H. Green, and C. H. Mody. 2002. Primary dendritic cells phagocytose *Cryptococcus neoformans* via mannose receptors and Fcγ receptor II for presentation to T lymphocytes. *Infect. Immun.* 70: 5972–5981.
43. Wozniak, K. L., J. M. Vyas, and S. M. Levitz. 2006. In vivo role of dendritic cells in a murine model of pulmonary cryptococcosis. *Infect. Immun.* 74: 3817–3824.
44. Powell, K. E., B. A. Dahl, R. J. Weeks, and F. E. Tosh. 1972. Airborne *Cryptococcus neoformans*: particles from pigeon excreta compatible with alveolar deposition. *J. Infect. Dis.* 125: 412–415.

DNA Research 15, 253–265, (2008) doi:10.1093/dnares/dsn014

Expression Profiling of PBMC-based Diagnostic Gene Markers Isolated from Vasculitis Patients

Shigeto Kobayashi[1], Akihiko Ito[2], Daisuke Okuzaki[3,4], Hiroaki Onda[3,5], Norikazu Yabuta[3], Ippei Nagamori[3], Kazuo Suzuki[6,7], Hiroshi Hashimoto[1], and Hiroshi Nojima[3,4,5,*]

Department of Rheumatology and Internal Medicine, Juntendo University School of Medicine, 2-1-1 Hongo, Bunkyo-ku, Tokyo 113-8421, Japan[1]; Division of Molecular Pathology, Department of Cancer Biology, Institute of Medical Science, The University of Tokyo, 4-6-1 Shirokanedai, Minato-ku, Tokyo 108-8639, Japan[2]; Department of Molecular Genetics, Research Institute for Microbial Diseases, Osaka University, 3-1 Yamadaoka, Suita, Osaka 562-0031, Japan[3]; DNA-chip Development Center for Infectious Diseases, Research Institute for Microbial Diseases, Osaka University, 3-1 Yamadaoka, Suita, Osaka 562-0031, Japan[4]; Innovation Plaza Osaka, Izumi, Osaka 594-1144, Japan[5]; Department of Bioactive Molecules, National Institute of Infectious Diseases, 1-23-1 Toyama, Shinjuku-ku, Tokyo 162-8640, Japan[6] and Inflammation Program, Department of Immunology, Chiba University, Graduate School of Medicine, Inohana 1-8-1 Chuo-ku, Chiba, 260-8670, Japan[7]

(Received 8 May 2008; accepted on 29 May 2008; published online 17 June 2008)

Abstract

Vasculitis (angiitis) is a systemic autoimmune disease that often causes fatal symptoms. We aimed to isolate cDNA markers that would be useful for diagnosing not only vasculitis but also other autoimmune diseases. For this purpose, we used stepwise subtractive hybridization and cDNA microarray analyses to comprehensively isolate the genes whose expressions are augmented in peripheral blood mononuclear cells (PBMCs) pooled from vasculitis patients. Subsequently, we used quantitative real-time polymerase chain reaction (qRT–PCR) to examine the mRNA levels of each candidate gene in individual patients. These analyses indicated that seven genes exhibit remarkably augmented expression in many vasculitis patients. Of these genes, we analyzed G0/G1 switch gene 2 (G0S2) further because G0S2 expression is also enhanced in the PBMCs of patients with systemic lupus erythematodes (SLE). We generated G0S2 transgenic mice that ubiquitously overexpress human G0S2. Although we did not observe any obvious vasculitis-related histopathologic findings in these mice, these mice are unhealthy as they produce only few offspring and showed elevated serum levels of two autoimmunity-related antibodies, anti-nuclear antibody, and anti-double strand DNA antibody. Thus, our large-scale gene profiling study may help finding sensitive and specific DNA markers for diagnosing autoimmune diseases including vasculitis and SLE.

Key words: vasculitis; angiitis; G0S2; EGR1; amphiregulin; hemoglobin delta

1. Introduction

There are ~10 different disorders that are classified as vasculitis (also known as angiitis). Vasculitis is a systemic autoimmune disease characterized by the chronic inflammation of systemic blood vessels, veins, and arteries of all types and sizes. This often causes symptoms that can rapidly induce death, such as the formation of blood clots (thrombosis), restriction of oxygenated blood supply (ischemia), and irreversible injury to affected organs.[1] Although immune system disturbances appear to be the main cause of the disease, the pathogenesis of vasculitis is not fully understood. The diagnosis and treatment of vasculitis was

Edited by Mitsuo Oshimura.

* To whom correspondence should be addressed.
Tel. +81 6-6875-3980. Fax. +81 6-6875-5192.
E-mail: snj-0212@biken.osaka-u.ac.jp

recently greatly aided by the observation that three vasculitis disorders, namely Wegener's granulomatosis (WG), microscopic polyangiitis (MPA), and Churg–Strauss syndrome (CSS), are characterized by the presence of circulating antineutrophil cytoplasmic antibodies (ANCAs).[2,3] Two different types of ANCA have been identified. C-ANCA targets proteinase-3 and is most frequently found in WG, whereas P-ANCA, which targets myeloperoxidase, is most frequently detected in MPA and CSS. Consequently, enzyme immunosorbent assays (EIA) that examine the ability of patient serum to bind to these enzymes can be used to diagnose WG, MPA, and CSS. However, diagnoses made on the basis of positive EIAs will still need to be confirmed by biopsies. Moreover, many other vasculitis disorders are not characterized by the presence of ANCAs. Thus, the diagnosis of vasculitis disorders requires the identification of more convenient and generally applicable diagnostic markers. The identification of these markers may also provide insights into the pathogenesis behind this disorder and improve the therapy of vasculitis.

We have isolated putative gene markers that are characteristic to the autoimmune diseases, such as systemic lupus erythematodes (SLE)[4] and rheumatoid arthritis (RA)[5], using peripheral blood mononuclear cells (PBMCs). Here, we sought to identify new gene markers that can distinguish the autoimmune disease, in particular vasculitis, from other diseases with high specificity when PBMCs serve as the sample. For this purpose, we used the stepwise subtraction technique[6] and high-density oligonucleotide microarrays to isolate those genes that show dramatically upregulated expression commonly in the pooled PBMC mRNAs of varieties of vasculitis patients regardless of the patient's symptom, active, or inactive phase when compared with normal volunteer PBMC mRNAs. To identify the genes that are upregulated in many vasculitis patients, we selected and mixed the PBMC mRNAs from patients with one of the following seven vasculitis disorders: WG, MPA, Takayasu's arteritis (TA), allergic granulomatous angiitis (AGA), malignant RA (MRA = rheumatoid vasculitis), giant cell arteritis (GCA), and polyarteritis nodosa (PN). We found that the following seven genes are commonly unpregulated in the PBMCs of many of these vasculitis patients regardless of their symptoms: early growth response 1 (*EGR1*), G0/G1 switch gene 2 (*G0S2*), hemoglobin delta (*HBD*), amphiregulin (also known as *AREG*), interleukin-1 receptor type II (*IL1R2*), *calgranulin C*, and a novel gene named *TVAS10*. Of these genes, we selected *G0S2* for further analysis because its physiological functions are poorly understood. We prepared anti-G0S2 antibodies and then generated G0S2 transgenic mice and examined their phenotype. We propose that the vasculitis gene markers we identified here may be useful for the future diagnosis of vasculitis.

2. Materials and methods

2.1. *Human subjects and ethical considerations*

All systemic vasculitis patients used in this study were diagnosed according to a previously documented proposal (the ACR criteria and the CHCC criteria).[1] This study was reviewed and approved by the Internal Review Board of the Research Institute for Microbial Diseases, Osaka University. Accordingly, written informed consent was obtained from all participants before their PBMCs were obtained. Serum samples were consecutively obtained regardless of the patient's symptom, active, or inactive phase.

2.2. *Statistical analysis*

Significant differences were determined by using Mann–Whitney *U*-test (Figs. 1 and 2B, Supplementary Fig. S1). The data are expressed as means $\pm$ SE. *P*-value of <0.05 or <0.01 was considered to be statistically significant.

2.3. *Transgene vector construction and production of G0S2 transgenic mice*

To construct the transgene vector pCX-G0S2, the human G0S2 ORF was cloned from a SLE cDNA library[4] by PCR with the *Eco*RI site-bearing primers G0S2-*Eco*RI-5'F (5'-TATGAATTCGCCACCATGGAAACGG TCCAGGAGCTGATC-3') and G0S2-*Eco*RI-3'R (5'-ATA GAATTCCTAGGAGGCGTGCTGCCGGTTGGAC-3'). The G0S2-*Eco*RI-5'F primer contains the Kozak sequence ahead of the start codon of G0S2 cDNA, whereas the G0S2-*Eco*RI-3'R primer contains the stop codon of G0S2 cDNA. The sequence of the amplified product was confirmed by DNA sequencing. As previously described,[7] the *Eco*RI-digested fragment of the amplified G0S2 ORF was inserted into the *Eco*RI site of the pCAGGS expression vector, which possesses a chicken β-actin promoter and a cytomegalovirus enhancer (CMV-IE enhancer). The resulting construct was designated pCX-G0S2. To prepare the G0S2 fragment bearing the chicken β-actin promoter and the CMV-IE enhancer for injection into fertilized eggs, the *Sal*I/*Hind*III fragment of pCX-G0S2 was purified by electrophoresis and agarose gel extraction. The G0S2 transgenic embryos and mice were generated according to previously described protocols.[7] Briefly, the purified DNA fragments were injected into B6D2F1 × B6D2F1 fertilized eggs. The incorporation of the transgene was examined by the genomic PCR analysis using DNA extracted from the tail and the pCX-G0S2-1685F (5'-GCTGGTTGTTGTGCTG TCTCATCA-3') and pCX-G0S2-2161R (5'-GCCAG

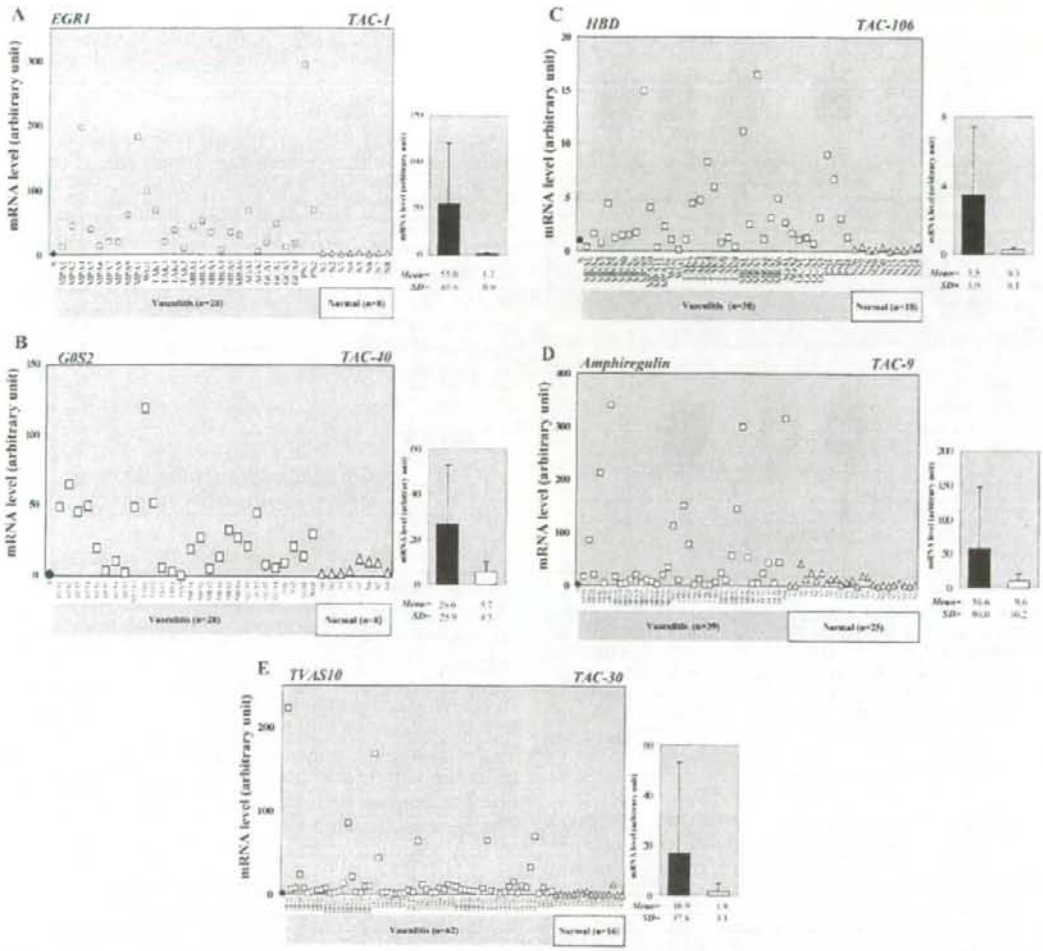

Figure 1. mRNA expression of selected *TAS/TAC* genes in the PBMCs from individual vasculitis patients and normal volunteers. qRT–PCR analyses show that (**A**) *EGR1* (*TAC-1*), (**B**) *G0S2* (*TAC-40*), (**C**) *HBD* (*TAC-106*), (**D**) *Amphiregulin* (*TAC-9*), and (**E**) *TVAS10* (*TAC-30*) are generally upregulated in the PBMCs of vasculitis patient (circles) but not in the PBMCs of normal volunteers (triangles). Each symbol denotes the mean value of a sample analyzed in triplicate. The leftmost filled circle signifies an RNA sample from the PBMCs of a healthy volunteer (male, age 52), which was used as a standard sample and whose expression level was set to 1.0. It allowed us to compare all of the expression profiles tested in this study. Average ± SE values of the vasculitis patient and normal volunteer groups are shown in the right-hand graphs and differ significantly ($P < 0.01$).

AAGTCAGATGCTCAAGGGGCTTCA-3′) primers. The PCR conditions involved TaKaRa Ex *Taq* polymerase (Takara, Shiga, Japan) and a pre-heating step (95°C for 2 min), 30 reaction step cycles (95°C for 30 s, 58°C for 30 s, 72°C for 1 min), and a final elongation step (72°C for 5 min). The founder mice were mated with C57BL/6 mice and both the transmittance of the transgene and the successful expression of human G0S2 protein were examined by western blot analysis of total cell extracts of mouse tails using one of the anti-G0S2 monoclonal antibodies (clone #3-1) we generated (see section 3.4 and Supplementary Fig. S2).

2.4. *Histological examination*

C57BL/6 mice were purchased from Japan SLC (Hamamatsu, Japan). Mouse tissues were fixed immediately after removal with 4% paraformaldehyde, then embedded in paraffin, and cut into sections (4 μm

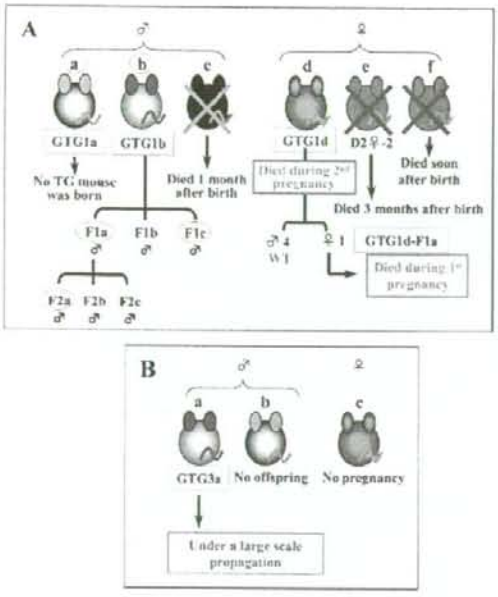

Figure 2. Family tree of *G0S2* transgenic mice. (**A**) Of the 61 mice tested in the first trial, six *G0S2* transgenic mouse lines were generated. They all died except for the GTG1b line, which was not useful for further analysis because the human G0S2 gene was introduced on the Y chromosome; consequently, this mouse only produced male *G0S2* transgenic mice. (**B**) Of the 22 mice tested in the third trial, three *G0S2* transgenic mouse lines were generated. The only surviving GTG3a line is now under large scale propagation to establish a strain.

thick). Some sections were stained with hematoxiln and eosin according to standard procedures, whereas others were stained with the clone #3-1 monoclonal anti-G0S2 antibody according to the previously described procedure.[8] To evaluate the immunostain, sections of the same organs from G0S2-TG and C57BL/6 mice were processed at the same time. When the immunoreactive signals in the former sections were substantially stronger than those in the latter, they were considered to indicate the exogenic G0S2 proteins produced from the transgene.

2.5. *In situ hybridization*

Sections were processed in the Genostaff laboratory (Tokyo, Japan) by using the DIG RNA labeling and detection kits (Roche Diagnostics, Mannheim, Germany). Briefly, G0S2 antisense and sense (negative control) RNA probes were prepared by *in vitro* transcription of the pBluescript vector containing the full-length human G0S2 cDNA according to the manufacturer's instructions. Hybridized signals were colored blue with 4-nitro blue tetrazolium chloride and 5-bromo-4-chloro-3-indolyl-phosphate as a substrate of alkaline phosphatase. The sense probe did not yield any significant stains. Further information concerning the *in situ* hybridization (ISH) method is available on request.

2.6. *Serologic examination*

Approximately 200 μl of peripheral blood per mouse were collected from the orbital plexus under anesthesia and were left for 1 h to coagulate. After centrifugation, ~20 μl sera were obtained. The sera were frozen at −20°C and sent to the Mitsubishi Kagaku BCL laboratory (Tokyo, Japan), where each serum was diluted 500 times and analyzed for the levels of anti-nuclear and anti-double strand (ds) DNA antibodies by fluorescent antibody tests or enzyme immunoassays.

3. Results

3.1. *Identification of vasculitis-specific genes by stepwise subtraction and DNA microarray analysis*

To isolate the putative vasculitis-specific genes that are commonly upregulated in the PBMCs of vasculitis patients, we first used our stepwise subtractive hybridization method. PBMC samples were obtained from vasculitis patients (50 patients in total) regardless of the patient's symptom, active, or inactive phase, and a cDNA library was prepared from their pooled mRNAs by the linker-primer method using a pAP3neo vector.[9] Stepwise subtractive hybridization was then performed using the biotinylated pooled mRNAs from the PBMCs of eight normal volunteers, as described previously.[6] This generated a library of genes that are upregulated in only vasculitis PBMCs. To examine whether these genes are actually upregulated in vasculitis but not normal PBMCs, we performed northern blot analysis using the pooled mRNAs from the vasculitis and normal PBMCs (Fig. 3A). For the cDNA clones whose expression levels were too low for detection by northern blot analysis, we examined their expression in vasculitis and normal PBMCs by RT–PCR (Fig. 3B). The 29 genes that were confirmed to be upregulated in vasculitis patients were called *TAS* after transcript augmented in vasculitis isolated by stepwise-subtraction. The *TAS* genes and their accession numbers are summarized in Table 1.

To increase the number of putative vasculitis-specific genes, we also performed a genome-wide complementary DNA microarray analysis using the Agilent Hu44K array with the same pooled vasculitis and normal PBMC RNA samples. When we tested the top 402 genes from the microarray list of vasculitis-upregulated genes (data not shown) by RT–PCR, we identified 63 genes whose expression levels are dramatically upregulated in vasculitis patient PBMCs

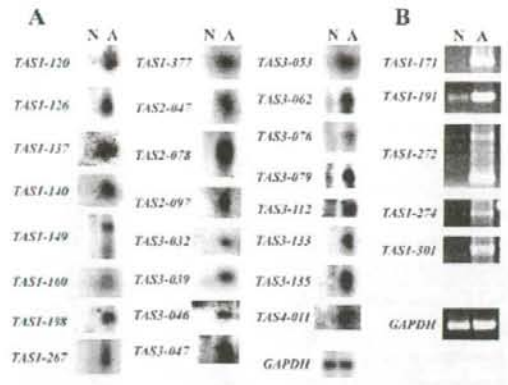

Figure 3. mRNA expression levels of the *TAS* genes. Individual *TAS* genes were subjected to northern blot (**A**) or RT–PCR (**B**) analysis to confirm they are upregulated in the PBMCs of 50 vasculitis patients (A) but not in the PBMCs of eight normal volunteers (N). Table 1 provides the names of the *TAS* genes. *GAPDH* was also analyzed as a loading control. The annealing temperature for RT–PCR was always 58°C and amplification occurred over 30 cycles. The sequences of the primers used to identify the *TAS* genes are presented in Supplementary Table S1.

(Fig. 4). We called them *TAC* after transcript augmented in vasculitis isolated by cDNA-microarray. The *TAC* genes and their accession numbers are summarized in Table 2. Dual specificity phosphatase 1 (*DUSP1*) and *IL1R2* were identified by both methods. Of the 92 *TAS* and *TAC* genes, 30 genes are uncharacterized genes. These are designated as *TVAS* after transcript increased in vasculitis.

3.2. *Expression profiles of vasculitis-upregulated genes in individual patients*

To determine whether these vasculitis-specific candidate genes are indeed upregulated in patients suffering from WG, MPA, TA, AGA, MRA, GCA, or PN and thus are general markers of vasculitis, we subjected 25 of the *TAS* and *TAC* genes (underlined in Tables 1 and 2) to quantitative RT–PCR (qRT–PCR) using PBMC RNA samples from indicated numbers of individual vasculitis patients and normal volunteers as negative controls (Fig. 1 and Supplementary Fig. S1). In every qRT–PCR, a standard RNA (denoted as normal with a relative intensity of 1.0) from the PBMCs of a healthy volunteer (male, age 52) was used (see the leftmost filled circle in Fig. 1A–E); this allowed us to compare the expression profiles of the genes tested in this study. It also allowed us to compare the expression profiles of the genes in this study with those of other genes tested in our previous studies on SLE[4] and RA.[5] With this experiment, we expected to isolate those genes that are highly expressed not only in many vasculitis patients but also in patients with SLE[4] and RA;[5] the identification of such marker genes may be useful as sensitive and specific diagnostic tools.

Of the 25 *TAS/TAC* genes tested, *TAC-1* [early growth responses 1 (*EGR1*)] was one of the most strongly upregulated genes commonly in the PBMCs of many vasculitis patients, as 96% of patients expressed this gene at 3–300-fold higher levels than healthy volunteers (Fig. 1A). *EGR1* encodes a zinc finger transcription factor whose expression is induced within minutes upon the reception of growth stimuli; its expression then decays within a few hours. It promotes cellular differentiation along a macrophage lineage.[10] It also plays a critical role in the response to both acute and chronic vascular stress by inducing the expression of several gene products linked to cellular perturbation. This is particularly true for the cellular perturbation in the vasculature that is induced by hypoxia, ischemia/reperfusion, atherosclerosis, and acute vascular injury.[11] It remains unclear whether the induction of *EGR1* in vasculitis is a pathogenic response or merely results from vascular stress. Nonetheless, *EGR1* may serve as a gene marker for the diagnosis of vasculitis.

TAC-40 (*G0S2*) is a lymphocyte G0/G1 switch gene that encodes a putative cell cycle inhibitor whose expression may be required before cells become committed to enter the G1 phase of the cell cycle.[12] Nearly, half of the vasculitis patients showed >20-fold increased expression, whereas the expression of most of the normal volunteers was much lower (Fig. 1B). Notably, relative to healthy controls, *G0S2* expression is also enhanced in the PBMCs from patients with other autoimmune diseases, namely SLE[4] and RA.[5] Microarray and qRT–PCR analyses also showed that *G0S2* is upregulated in the PBMCs from psoriasis patients suffering from severe generalized disease.[13] Thus, it may be interesting to analyze *G0S2* further, as it may shed light on the pathogenesis of vasculitis at the molecular level (see below).

Nearly 77% of the vasculitis patients expressed 3–16-fold more *TAC-106* (*HBD*) mRNA than the normal volunteers (Fig. 1C). HBD is a minor type of hemoglobin (it makes up only 2–3% of adult hemoglobin) that forms a complex with α-hemoglobin called hemoglobin A_2 ($\alpha_2\delta_2$).[14] Although high HbA2 levels are diagnostic for the β-thalassemia trait, its relevance to vasculitis pathology is unknown. Nonetheless, it may be useful as a diagnostic gene marker for vasculitis.

Amphiregulin is one of the epidermal growth factor (EGF)-like growth factors that stimulate cell growth by activating the EGF receptor signaling of target cells in an autocrine/juxtacrine fashion.[15] We previously reported that *Amphiregulin* expression is enhanced in the PBMCs of some patients with SLE[4] and RA.[5]

Table 1. List of stepwise subtraction identified *TAS* genes that show upregulated expression in vasculitis patient PBMCs

Gene name	Accession number	Sequence description
TAS1-120	AK091533	Unknown (sapiens cDNA FLJ34214) = *TVAS1*
TAS1-126	NM_006013	Ribosomal protein L10 (RPL10)
TAS1-137	AC007318	Unknown (AL049356) = *TVAS2*
TAS1-140	BC033089	Lipocalin 2 (oncogene 24p3)
TAS1-149	BC008684	Similar to splicing factor, arginine/serine-rich (MGC:9742)
TAS1-160	NM_016304	Unknown (C15orf15) = *TVAS3*
TAS1-198	BC010878	ASF1 anti-silencing function 1 homolog A
TAS1-267	BC042436	Unknown (IMAGE:4471726) = *TVAS4*
TAS1-377	AY275537	Unknown (isolate 183 mitochondrion) = *TVAS5*
TAS2-047	BC047681	S100 calcium binding protein A9 (calgranulin B)
TAS2-078	NM_004417	Dual specificity phosphatase 1 (DUSP1)
TAS2-097	D89974	Glycosylphosphatidyl inositol-anchored protein GPI-80
TAS3-032	NM_015384	Nipped-B homolog (*Drosophila*) (NIPBL)
TAS3-039	NM_001030	Ribosomal protein S27 (metallopanstimulin 1) (RPS27)
TAS3-046	BC000927	Poly(A) polymerase alpha
TAS3-047	NM_000517	Hemoglobin, alpha 2 (HBA2)
TAS3-053	NM_004633	Interleukin 1 receptor, type II (IL1R2)(AY124010)
TAS3-062	BC000163	Vimentin
TAS3-076	BC064910	Beta-2-microglobulin
TAS3-079	BC001429	Annexin A5
TAS3-112	AY195792	Unknown (haplotype As9Y mitochondrion) = *TVAS6*
TAS3-133	NM_005870	Sin3-associated polypeptide, 18kDa (SAP18)
TAS3-135	BC018183	NADH dehydrogenase (ubiquinone) 1 beta subcomplex
TAS4-011	CR611844	Unknown (CS0DL007YO12 of B cells) = *TVAS7*
TAS1-171	AY260957	Insulin-like growth factor 1 (somatomedin C) (IGF1)
TAS1-191	NM_005621	S100 calcium-binding protein A12 (calgranulin C)
TAS1-272	NM_003805	CASP2 and RIPK1 domain containing adaptor with death domain (CRADD)
TAS1-274	NM_004592	Splicing factor, arginine/serine-rich 8 (SFRS8)
TAS1-301	BC062616	Protein serine kinase H1

The expression levels of the *TAS* genes were examined by northern blot (Fig. 1A) and/or RT–PCR (Fig. 1B). The underlined genes were subjected to qRT–PCR to determine their generality of expression in vasculitis patients but not normal volunteers (Fig. 3).

However, compared with SLE and RA patients, a far smaller proportion of vasculitis patients show enhanced *Amphiregulin* expression (Fig. 1D). Thus, *Amphiregulin* may be more significant as a DNA marker for SLE and RA than for vasculitis.

TAC30 (=*TVAS10*) encodes an uncharacterized novel protein that is composed primarily of an ankyrin repeat, which is one of the most frequently observed amino-acid motifs and is important for protein–protein interactions.[16] About a half of the vasculitis patients showed 10–200-fold increased expression of *TAC30*, whereas healthy volunteers showed very low expression except for one case (Fig. 1E).

Interleukin-1 (IL1), a principal macrophage-derived cytokine, plays a pivotal role in the immuno-inflammatory process by triggering cell activation *via* its type I receptor (IL1R1); in contrast, its type II receptor (IL1R2) lacks the intracellular domain for IL1 signaling and functions as a potent, specific, and natural inhibitor of IL1 by acting as a decoy receptor.[17] About half of the vasculitis patients showed 20–50-fold *IL1R2* expression (one patient showed ~300-fold expression), whereas healthy volunteers showed very low expression except for one case (Supplementary Fig. S1A). This increased expression of IL1R2 may be related to the vascular inflammation of the vasculitis patients.

Three phagocyte-specific S100 proteins called calgranulin- A, -B, and -C act separately during calcium-dependent signaling. In particular, *TAS1-191* (*calgranulin C*) secretion by tumor necrosis factor (TNF)- stimulated granulocytes causes target cell activation that results in the upregulated expression of proinflammatory

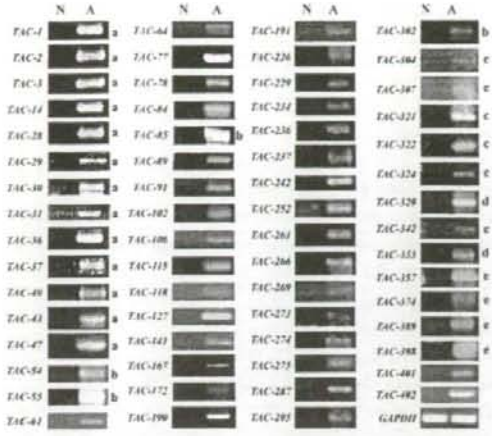

Figure 4. mRNA expression levels of the *TAC* genes. Individual *TAC* genes were subjected to RT–PCR analysis to confirm they are upregulated in the PBMCs of 50 vasculitis patients (A) but not in the PBMCs of eight normal volunteers (N). GAPDH was also analyzed as a loading control. The annealing temperature and amplification cycles for RT–PCR were always 50°C and 35 cycles, respectively, with the exception of the reactions denoted by a (55°C, 40 cycles), b (50°C, 30 cycles), c (58°C, 27 cycles), d (50°C, 40 cycles), and e (58°C, 30 cycles). The sequences of the primers used to identify the *TAS* genes are presented in Supplementary Table S1.

cytokines such as TNF and IL1β; the TNF that is released may then stimulate granulocytes to secrete more calgranulin C, thereby establishing a self-amplifying positive feedback loop.[18] About 30% of vasculitis patients showed 10–50-fold *calgranulin C* expression (one patient showed ~150-fold expression), whereas most of the healthy volunteers showed low expression (Supplementary Fig. S1B). In contrast, the vasculitis patients and normal volunteers did not differ in their expression of *calgranulin B* (*TAS2-047*) (data not shown).

3.3. *Expression pattern of TAS/TAC genes in PBMC*

We previously reported that *G0S2* was primarily expressed in monocytes, whereas *Amphiregulin* was expressed in both monocytes, T cells and B cells by performing RT–PCR on multiple-tissue cDNA panels (MTC) from Clontech (Palo Alto, CA).[5] To determine whether *EGR1*, *HBD*, *TVAS10*, *IL1R2*, and *calgranulin C* are also expressed in particular human blood cells, we conducted similar experiments. As shown in Fig. 5, *EGR1* and *IL1R2* were expressed ubiquitously in all lanes, albeit with varying intensities. cDNA from placenta, which also contains many blood cells, served as a control. All genes except *calgranulin C* were strongly expressed in activated $CD4^+$ T cells (lane 8) and weakly expressed in activated mononuclear cells (aMNCs) (lane 7). Only *EGR1* and *TVAS10* were expressed in activated $CD8^+$ T (lane 9) cells. *EGR1*, *TVAS10*, *IL1R2*, and *calgranulin C* were expressed in resting $CD8^+$ T cells (T-suppressor/cytotoxic; lane 2) and monocytes (lane 4). These observations together indicate that these vasculitis-upregulated genes have similar expression profiles. Unfortunately, we could not perform this analysis on vasculitis patients because of the low numbers of PBMCs that we could obtain from the patients.

3.4. *Preparation of transgenic mice that overexpress G0S2*

We selected G0S2 for further analysis because little is known about its physiological significance and function. To explore the physiological significance of G0S2, we prepared transgenic mice that overexpress the human gene for G0S2. For this purpose, we constructed plasmid DNA in which human G0S2 cDNA lies directly downstream of the beta-actin promoter, as described previously.[7] This construct was used to generate transgenic mouse lines that express human G0S2 protein in all tissues. The successful generation of these transgenic mice was confirmed by PCR and/or western blot analysis using DNA or cell extracts obtained from the tail. Expression of G0S2 protein was confirmed by the monoclonal antibody (#3-1) we prepared here (see Supplementary Result and Fig. S2). Although the transgenic mice did not exhibit an obvious phenotype, they seemed to be unhealthy as they did not produce large numbers of offspring. This made it very difficult to establish this transgenic mouse line. For example, in the first attempt to generate this line, 61 mice were tested by PCR for expression of human G0S2. Of these, three female and three male mice were found to bear the transgene (GTG1a-f, see Fig. 2). However, the GTG1f female mouse died soon after birth and the GTG1e female and GTG1c male mice died 3 and 1 months after birth, respectively (Supplementary Fig. S4A). Moreover, while the surviving female transgenic mouse (GTG1d) produced one female transgenic mouse, which safely grew to adulthood, the mother died during her next pregnancy. Her daughter also died during her first pregnancy. In addition, the surviving male mouse GTG1b only produced male transgenic mice when mated with wild-type B6 female mice because the human G0S2 gene was introduced into the Y chromosome. Thus, this mouse could not be used further. Furthermore, the remaining surviving male mouse, GTG1a, did not produce transgenic mouse when mated with wild-type B6 female mice. Thus, we failed to establish a human G0S2-expressing transgenic strain in this trial. The second trial did not generate any transgenic mice. However, in the third trial, of the 22 mice examined by PCR (Fig. 6A) and western blot analysis (Fig. 6B), we found three

Table 2. List of microarray identified *TAC* genes that show upregulated expression in the PBMCs of vasculitis patients

Gene name	Accession number	Sequence description
TAC-1	NM_001964	Early growth response 1 (EGR1) gene product
TAC-2	AK025198	Unknown (FLJ21545) = *TVAS8*
TAC-3	NM_000584	Interleukin 8 (IL8)
TAC-9	NM_001657	Amphiregulin
TAC-14	NM_003596	Tyrosylprotein sulfotransferase 1 (TPST1)
TAC-19	NM_004633	Interleukin 1 receptor, type II (IL1R2)
TAC-28	NM_000715	Complement component 4 binding protein, alpha (C4BPA)
TAC-29	NM_017762	Unknown (FLJ20313) = *TVAS9*
TAC-30	NM_144590	Unknown (ankyrin repeat domain 22: MGC22805) = *TVAS10*
TAC-31	BC013734	Prostaglandin-endoperoxide synthase 2
TAC-36	AB044805	6-phosphofructo-2-kinase heart isoform
TAC-37	NM_001511	Chemokine (C-X-C motif) ligand 1 (CXCL1)
TAC-40	NM_015714	G0/G1 switch gene 2 (G0S2)
TAC-43	NM_004545	NADH dehydrogenase (ubiquinone) 1 beta (NDUFB1)
TAC-47	NM_080657	Viperin (cig5)
TAC-54	BC029495	Unknown (MGC:33104) = *TVAS11*
TAC-55	AF249277	Cervical cancer suppressor-1
TAC-61	BC065737	Unknown (IMAGE:30404477) = *TVAS12*
TAC-64	NM_000032	Aminolevulinate, delta-, synthase 2 (ALAS2)
TAC-77	NM_000661	Ribosomal protein L9 (RPL9)
TAC-78	NM_004233	CD83 antigen (immunoglobulin superfamily)
TAC-84	X60364	ALAS mRNA for 5-aminolevulinate synthase precursor
TAC-85	AK098605	Unknown (FLJ25739) = *TVAS13*
TAC-89	NM_004833	Absent in melanoma 2 (AIM2)
TAC-91	NM_001738	Carbonic anhydrase I (CA1)
TAC-102	NM_005143	Haptoglobin (HP)
TAC-106	BQ446275	Hemoglobin delta (HBD)
TAC-115	NM_182522	TAFA4 protein (TAFA4)
TAC-118	L03419	Fc-gamma receptor I B1
TAC-127	NM_007115	Tumor necrosis factor, alpha-induced protein 6 (TNFAIP6)
TAC-141	BX537874	Unknown (DKFZp313P036) = *TVAS14*
TAC-167	BQ674642	Unknown = *TVAS15*
TAC-172	AL390162	Unknown (DKFZp761A1916) = *TVAS16*
TAC-190	NR_001459	Unknown (C14orf62) = *TVAS17*
TAC-191	NM_002983	Chemokine (C-C motif) ligand 3 (CCL3)
TAC-226	BC031359	Unknown (IMAGE:4778855) = *TVAS18*
TAC-229	NM_002064	Glutaredoxin (thioltransferase) (GLRX)
TAC-234	NM_000963	Prostaglandin G/H synthase and cyclooxygenase (PTGS2)
TAC-236	NM_001124	Adrenomedullin (ADM)
TAC-237	NM_014320	Heme-binding protein 2 (HEBP2)
TAC-242	AW901958	Unknown = *TVAS19*
TAC-252	NM_003096	Small nuclear ribonucleoprotein polypeptide G (SNRPG)
TAC-261	NM_014879	G protein-coupled receptor 105 (GPR105)
TAC-266	BC032663	Phorbol-12-myristate-13-acetate-induced protein 1
TAC-269	BC032480	Unknown (IMAGE:5214272) = *TVAS20*
TAC-273	NM_182619	Secretory protein LOC348174 (LOC348174)
TAC-274	NM_012472	Testis specific leucine rich repeat protein (TSLRP)

Continued

Table 2. Continued

Gene name	Accession number	Sequence description
TAC-275	AX721252	Unknown (Patent WO0220754) = *TVAS21*
TAC-287	NM_032412	Putative nuclear protein (ORF1-FL49)
TAC-295	NM_024850	Butyrophilin-like 8 (BTNL8)
TAC-302	BC005984	Unknown (IMAGE:4247211) = *TVAS22*
TAC-304	NM_033655	Unknown = *TVAS23*
TAC-307	BC042517	Unknown (IMAGE:4822953) = *TVAS24*
TAC-321	AL831953	Unknown (DKFZp667P0410) = *TVAS25*
TAC-322	AK128746	Unknown (FLJ44672) = *TVAS26*
TAC-324	AF067801	Unknown (HDCGC21P) = *TVAS27*
TAC-330	D86962	Unknown (KIAA0207) = *TVAS28*
TAC-343	NM_004417	Dual specificity phosphatase 1 (DUSP1)
TAC-353	M64109	Udulin 2
TAC-357	BC053669	Unknown (IMAGE:6146402) = *TVAS29*
TAC-374	NM_016220	Zinc finger protein (ZFD25)
TAC-389	NM_001955	Endothelin 1 (EDN1)
TAC-398	NM_020995	Haptoglobin-related protein (HPR)
TAC-401	NM_001161	Nudix (nucleoside diphosphate linked moiety X)-type motif 2 (NUDT2)
TAC-402	AY358224	Unknown (UNQ9368) = *TVAS30*

The expression levels were examined by RT–PCR (Fig. 2). The underlined genes were subjected to qRT–PCR to determine their generality of expression in vasculitis patients but not normal volunteers (Fig. 3).

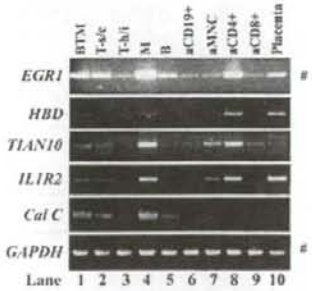

Figure 5. Determination of the human blood cells that express *EGR1*, *HBD*, *TVAS10*, *IL1R2*, and *calgranulin C* (*Cal C*). RT–PCR was performed by using the multiple-tissue cDNA panel for human blood fractions (MTC, Clontech). *GAPDH* was also amplified as a loading control. PCR amplifications were conducted at 50°C over 33 cycles except as indicated at the right of the panels by # (50°C over 30 cycles). Lane 1, mononuclear cells (B, T cells, and monocytes). Lane 2, resting CD8+ cells (T-suppressor/cytotoxic cells). Lane 3, resting CD4+ cells (T-helper/inducer). Lane 4, resting CD14+ cells (monocytes). Lane 5, resting CD19+ cells (B cells). Lane 6, activated CD19+ cells (aCD10+). Lane 7, activated mononuclear cells (aMNC). Lane 8, activated CD4+ cells (aCD8+). Lane 9, activated CD8+ cells. Lane 10, human placenta, which also includes many blood cells. The latter lane served as a control.

transgenic mice, of which one (GTG3a) produced offspring (see Supplementary Fig. S4B). These mice appear to be healthier than the other transgenic mice and consequently we have been able to maintain this line probably due to lower G0S2 levels than other transgenic mice. Thus, the exogenous and ubiquitous overexpression of human G0S2 seems to make the transgenic mice unhealthy and inhibits their production of offspring.

3.5. *Human G0S2 expression patterns in transgenic mice*

To examine the expression patterns of exogenous human G0S2 in various transgenic mouse tissues, we first performed ISH analysis. As shown in some representative pictures (Fig. 6C), high-level expression of *G0S2* mRNA was detected in various organs and tissues. The signals in the urinary tubule, gastric foveola, and esophageal mucosa were distributed in epithelial clumps (Fig. 6Ci–iii). In contrast, scattered or diffusely distributed signals were detected in the cardiac ventricle, gastric smooth muscle, and seminiferous tubule (Fig. 6Civ–vi).

Immunohistochemical analysis using the monoclonal antibody (#3-1) also detected exogenously expressed human G0S2 proteins in various organs and tissues of the transgenic mice. As shown in some representative pictures (Fig. 6D), the cellular distribution pattern of these proteins was similar to that of exogenous *G0S2* mRNA (Fig. 6C). In the kidney, although most urinary tubule epithelia were

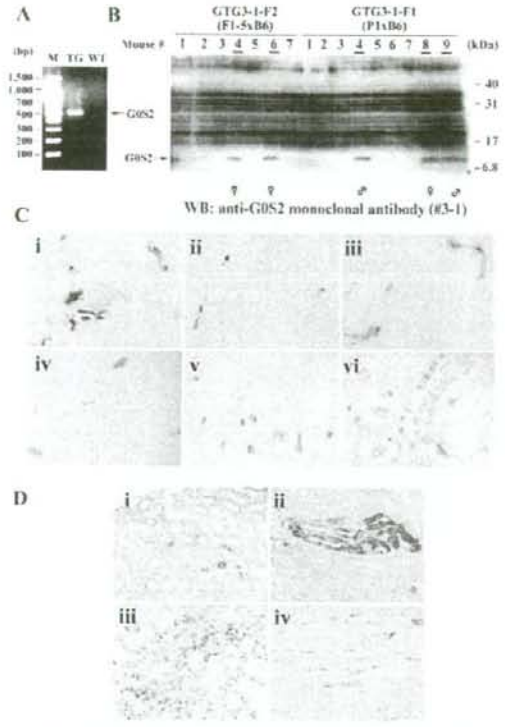

Figure 6. Establishment of *G0S2* transgenic mice. (**A**) An example of the RT–PCR analyses used to identify *G0S2* transgenic mice. (**B**) Western blot analysis to identify *G0S2* transgenic mice. The panel for ATG3-F1 and -F2 mice is shown as an example. The transgenic mouse numbers are underlined. (**C**) ISH analyses of G0S2-TG mice. Sections from the kidney (i), stomach (ii, mucosa; v, smooth muscle), esophagus (iii), heart (iv), and epididymis (vi) of adult G0S2-TG mice (GTG1b is shown as an example) were hybridized with the human G0S2 antisense probe and colored blue by using the alkaline phosphatase reaction. The nuclei were counterstained with nuclear fast red. Original magnification: ×200. (**D**) Immunological detection of exogenic G0S2 proteins in various organs of G0S2-TG mice (GTG1b is shown as an example). Sections from the kidney (i), stomach (ii), lung (iii), and heart (iv) of the adult G0S2-TG mice were incubated with the mouse monoclonal anti-G0S2 antibody (#3-1) and stained with diaminobenzidine. The nuclei were counterstained with hematoxylin. Original magnification: **A** and **B**, ×200; **C** and **D**, ×400.

weakly positive for G0S2, other epithelia expressed this protein at high levels; the latter epithelia also existed in clumps (Fig. 6Di). A similar patchy distribution of strong G0S2 signals was detected in the foveolar epithelia of the stomach (Fig. 6Dii). In the lung and heart, there was a scattered distribution of exogenous G0S2 signals in the alveolar epithelium and a diffuse distribution in cardiac ventricular muscle, respectively (Fig. 6Diii and iv).

3.6. *Phenotypes of G0S2 transgenic mice*

To explore the phenotypes of the G0S2 transgenic mouse, we first subjected various organs of G0S2 transgenic mice and wild-type (C57BL/6) mice to histological examination. Obvious histopathological findings that related directly to vasculitis were not observed. Notably, microabscess-like panniculitis lesions were detected in the dermis and subcutaneous fat tissue (Fig. 7A). Of the eight TG mice examined, such lesions were detected in three. We also measured the serum levels of two autoimmunity-related antibodies, namely, anti-nuclear antibody (ANA) and anti-dsDNA antibody. We found both were increased in G0S2 TG mice: the OD490 for ANA in the transgenic mice was 0.359 ± 0.170 [compared with 0.219 ± 0.044 for wild-type (B6) mice], whereas the OD490 for anti-dsDNA antibody was 0.294 ± 0.090 (compared with 0.188 ± 0.038 in wild-type mice) (Fig. 7B). However, these differences did not reach statistical significance,

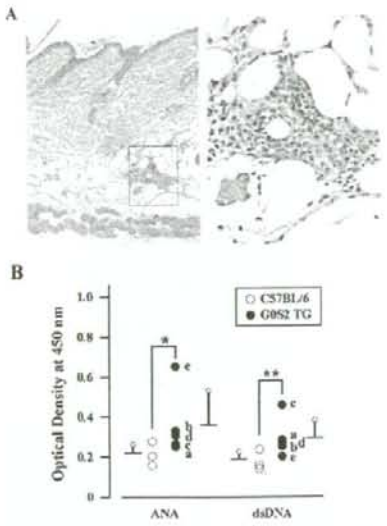

Figure 7. Histological and serological phenotypes of G0S2-TG mice. (**A**) Histological phenotype of G0S2-TG mice (GTG1b is shown as an example). Sections of the back skin of adult G0S2-TG mice were stained with hematoxylin and eosin. A boxed area in the left panel is enlarged in the right to show microabscess lesions containing numerous neutrophils. Original magnification: left, ×100; right, ×400. (**B**) Serological phenotypes of G0S2-TG mice (GTG1a is shown as an example). The sera from adult C57BL/6 (open circle) or G0S2-TG (closed circle) mice were examined for the levels of ANA and anti-dsDNA antibody. Asterisk and double asterisks indicate 'not significant' because $P = 0.1011$ and $P = 0.0526$, respectively, as determined by the Mann–Whitney *U*-test of differences between G0S2-TG and wild-type mice. The G0S2 TG mice examined are designated as follows: a (GTG1a), b (GTG1b), c (GTG1b-F1a), d (GTG1b-F2a), and e (GTG1b-F1c). The values of individual mice are plotted.

in part, because of the limited number of G0S2 TG mice we could use for these measurements. Taken together, it appears that G0S2 may participate in the pathogenesis of autoimmune diseases in general, and in particular, it may be related to inflammation.

4. Discussion

In the present study, we report candidate gene markers for vasculitis that may be useful for diagnosing and understanding the basic pathogenesis of vasculitis and other autoimmune diseases such as SLE. These genes were identified by stepwise subtraction and cDNA microarray techniques, which permitted us to comprehensively isolate the genes that show augmented mRNA expression in the PBMCs of vasculitis patients when compared with normal volunteers. The vasculitis-specific upregulation of these genes was validated with northern blot and/or RT–PCR analyses (Figs 3 and 4, Tables 1 and 2). We then showed by RT–PCR analysis that *EGR1*, *G0S2*, *HBD*, *TVAS10*, *IL1R2*, *Amphiregulin*, and *calgranulin C* are frequently upregulated in the PBMCs of vasculitis patients (Fig. 1 and Supplementary Fig. S1). MTC analysis revealed that in normal PBMCs, these genes are expressed primarily by monocytes and/or activated CD4+ cells (Fig. 5). We also showed previously using different primers and PCR conditions that *G0S2* is predominantly expressed by monocytes.[5] These results suggest that monocytes, including macrophages, express these vasculitis-upregulated genes and thus may play a role in the pathogenesis of vasculitis.

We noticed that several putative vasculitis-upregulated genes also show upregulated expression in other autoimmune diseases, namely, SLE and RA (Table 3). Of these, *EGR1* is particularly interesting as the degree to which it is upregulated in most vasculitis patients is remarkable (Fig. 1A). *EGR1* is induced by a variety of cellular stresses, including hypoxia, and may function as a master switch that triggers the expression of numerous key inflammatory mediators. In particular, *EGR1* induces a number of gene products that have been linked to cellular perturbation, especially in the vasculature. Moreover, many of these genes are often induced in the PBMCs of patients afflicted with a variety of autoimmune diseases. For example, we showed previously that *EGR1* is markedly upregulated in the PBMCs of SLE patients.[4] It also plays a critical role in promoting cellular differentiation along a macrophage lineage.[10] Nonetheless, *EGR1*-null mice are viable and develop and grow normally.[19] Rigorous analyses will be needed to determine whether the upregulation of *EGR1* mRNA in many vasculitis patients is pathogenically significant or merely an associated phenomenon.

G0S2 also displayed enhanced expression in many vasculitis patients (Fig. 1B). *G0S2* was first identified as one of the G0/G1 switch (G0S) genes that are differentially expressed in lymphocytes during their lectin-induced switch from the G0 to the G1 phases of the cell cycle.[20] *G0S2* is one of the genes that is upregulated during normal implantation but its expression is significantly lower in women with endometriosis that is associated with pelvic pain and infertility with implantation failure.[21] In a replicative senescence model employing human dermal fibroblasts (HDF), *G0S2* expression was upregulated in old HDF cells, which suggests that it participates in senescence.[22] Microarray and qRT–PCR analyses of

Table 3. List of the *TAC/TAS* genes that also show upregulated expression in PBMCs from SLE and RA patients

Name	Vasculitis	SLE	RA	Sequence description
TAC-1	42.0	44.7	nc	Early growth response 1 (EGR1)
TAC-2	41.7	24.1	nc	Unknown (FLJ21545) = *TVAS8*
TAC-3	29.7	23.2	2.4	Interleukin 8 (IL8)
TAC-9	12.3	12.3	27.4	Amphiregulin
TAC-13	9.7	11.3	1.8	CD69 antigen (early T-cell activation antigen)
TAC-14	9.4	7.2	3.9	Tyrosylprotein sulfotransferase 1 (TPST1)
TAC-19	9.1	5.3	9.4	Interleukin 1 receptor, type II (IL1R2)
TAC-20	8.8	18.0	1.4	Similar to interferon alpha-inducible protein 27
TAC-34	6.9	11.5	2.4	Sin3-associated polypeptide, 30kDa (SAP30)
TAC-37	6.8	3.9	2.4	Chemokine (C-X-C motif) ligand 1 (CXCL1)
TAC-40	6.7	14.8	4.0	G0/G1 switch gene 2 (G0S2)
TAC-47	6.4	20.7	nc	Viperin (cig5)
TAC-51	6.2	10.7	4.4	Nuclear factor of kappa B (NFκB)
TAC-78	5.5	11.4	1.7	CD83 antigen (immunoglobulin superfamily)

The numbers represent fold change compared with normal volunteers; nc, no conspicuous change between RA and control.

PBMCs from psoriasis patients suffering from severe generalized disease also revealed the upregulation of *G0S2*.[13] Moreover, we showed previously that *G0S2* mRNA levels are markedly increased in the PBMCs from patients with the autoimmune diseases SLE[4] and RA.[5] *G0S2* is a putative target gene of peroxisome-proliferator-activated receptor (PPAR) alpha, which belongs to a group of transcription factors that are involved in numerous processes, including lipid metabolism and adipogenesis. Moreover, it was shown that *G0S2* is upregulated after PPARδ activation and that it may be involved in the PPARδ-mediated mitigation of cardiac fibroblast proliferation.[23]

We here generated G0S2-TG mice that ubiquitously overexpress G0S2 proteins (Fig. 6). We showed that these mice are unhealthy as they do not produce many offspring (Fig. 2) and frequently display formations of microabscess-like panniculitis lesions in the dermis and subcutaneous fat tissue (Fig. 7A). The development of these microabscess-like panniculitis lesions may reflect the dysregulation of the murine immune system in these mice. Supporting this is that some of the G0S2-TG mice had augmented levels of immunodeficiency-related anti-nuclear and anti-dsDNA antibodies in their sera (Fig. 7B), although these phenotypes are related not to vasculitis but to SLE. It should be noted, however, that these serum differences did not achieve statistical significance, largely because of the shortage of G0S2-TG mice. It will be necessary to study larger numbers of G0S2-TG mice to confirm this association between *G0S2* overexpression and the development of autoimmune features. Should this association be confirmed, the high-quality polyclonal and monoclonal anti-G0S2 antibodies that we produced may be useful as tools (perhaps in enzyme-linked EIA) for diagnosing not just vasculitis but also other autoimmune diseases.

We performed this study on a highly heterogeneous cohort of patients, including those with systemic vasculitis. All of these diseases share the inflammatory involvement of blood vessels. However, their target organs, pathogenic mechanisms, clinical findings, and outcomes are quite different. Moreover, although the disease activity status in these patients was heterogeneous and some were receiving corticosteroid or immunosuppressive therapy, these factors were ignored in our patient recruitment protocol. Nonetheless, despite these marked heterogeneous features of our patient population, we could isolate putative common genes that are upregulated, which was our original goal. We are currently performing in parallel the expression profiling of the genes that are up- or downregulated in each individual disease and analyzing these profiles in terms of the symptoms, disease activity status, and clinical treatment of the patients. However, the results obtained from such studies are highly complex, which has hampered the identification of candidate gene markers that can be used for diagnosis.

Taken together, we conclude that the putative gene markers we identified here, in particular *EGR1* and *G0S2*, may be useful for diagnosing not only vasculitis but also other autoimmune diseases, perhaps by qRT–PCR and antibody-based methods. Other, as yet uncharacterized, genes that we detected as being upregulated in vasculitis may also be useful candidate gene markers and thus are worth further detailed analysis. In particular, the identification of the functions of these genes may reveal the hitherto unknown mechanism(s) that underlie the pathogenesis of vasculitis. This in turn may shed light on therapeutic avenues for treating vasculitis.

Acknowledgements: We thank the patients and healthy volunteers who participated in this study. We are obliged to Prof. Masaru Okabe, Prof. Masahito Ikawa, Ms Yumi Koreeda, Mr Masato Tanaka, Ms Yoko Esaki, Ms Akiko Kawai, and Ms Hisae Takema for useful advice and technical assistance in the generation of G0S2 transgenic mice. We also thank Ms Azumi Fujimori, Ms Chie Ishigami, Ms Ayami Ohtaka, Mr Akira Shigehisa, Dr Jun Sato, and Dr Takashi Kasama for technical assistance in the identification of *TAC* genes, and Dr Patrick Hughes for critically reading the manuscript.

Supplementary Data: Supplementary data are available online at www.dnaresearch.oxfordjournals.org.

Funding

This work was primarily supported by a grant-in-aid from the Health Science Research grant from the Ministry of Health and Welfare of Japan. This work was also supported in part by grants-in-aid to Hiroshi Nojima from Bio-Medical Cluster Project In Saito, Innovation Plaza Osaka and Regional Research and Development Resources Utilization Program of the Japan Science, and Technology Agency (JST), Scientific Research on Priority Areas "Applied Genomics", Scientific Research (S), Exploratory Research, and the Science and Technology Incubation Program in Advanced Regions from the Ministry of Education, Culture, Sports, Science, and Technology of Japan. Moreover, this study was partly supported by grants-in-aid to Kazuo Suzuki and Hiroshi Hashimoto from the Ministry of Health and Welfare of Japan.

References

1. Jennette, J. C., Falk, R. J., Andrassy, K., et al. 1994, Nomenclature of systemic vasculitides. Proposal of an

international consensus conference, *Arthritis Rheum.*, **37**, 187–192.
2. Selamet, U., Kovaliv, Y. B., Savage, C. O. and Harper, L. 2007, ANCA-associated vasculitis: new options beyond steroids and cytotoxic drugs, *Expert Opin. Investig. Drugs.*, **16**, 689–703.
3. Kallenberg, C. G. 2007, Antineutrophil cytoplasmic autoantibody-associated small-vessel vasculitis, *Curr. Opin. Rheumatol.*, **19**, 17–24.
4. Ishii, T., Onda, H., Tanigawa, A., et al. 2005, Isolation and expression profiling of genes upregulated in the peripheral blood cells of systemic lupus erythematosus patients, *DNA Res.*, **112**, 1–11.
5. Nakamura, N., Shimaoka, Y., Tougan, T., et al. 2006, Isolation and expression profiling of genes upregulated in bone marrow-derived mononuclear cells of rheumatoid arthritis patients, *DNA Res.*, **13**, 169–183.
6. Fujii, T., Tamura, K., Masai, K., Tanaka, H., Nishimune, Y. and Nojima, H. 2002, Use of stepwise subtraction to comprehensively isolate mouse genes whose transcription is up-regulated during spermiogenesis, *EMBO Rep.*, **3**, 367–372.
7. Ikawa, M., Kominami, K., Yoshimura, Y., Tanaka, K., Nishimune, Y. and Okabe, M. 1995, A rapid and non-invasive selection of transgenic embryos before implantation using green fluorescent protein (GFP), *FEBS Lett.*, **375**, 125–128.
8. Ito, A., Okada, M., Uchino, K., et al. 2003, Expression of the TSLC1 adhesion molecule in pulmonary epithelium and its downregulation in pulmonary adenocarcinoma other than bronchioloalveolar carcinoma, *Lab. Invest.*, **83**, 1175–1183.
9. Kobori, M., Ikeda, Y., Nara, H., et al. 1998, Large scale isolation of osteoclast-specific genes by an improved method involving the preparation of a subtracted cDNA library, *Genes Cells*, **3**, 459–475.
10. Nguyen, H. Q., Hoffman-Liebermann, B. and Liebermann, D. A. 1993, The zinc finger transcription factor Egr-1 is essential for and restricts differentiation along the macrophage lineage, *Cell*, **72**, 197–209.
11. Yan, S. F., Harja, E., Andrassy, M., Fujita, T. and Schmidt, A. M. 2006, Protein kinase C beta/early growth response-1 pathway: a key player in ischemia, atherosclerosis, and restenosis, *J. Am. Coll. Cardiol.*, **48**, A47–A55.
12. Cristillo, A. D., Heximer, S. P., Russell, L. and Forsdyke, D. R. 1997, Cyclosporin A inhibits early mRNA expression of G0/G1 switch gene 2 (G0S2) in cultured human blood mononuclear cells, *DNA Cell. Biol.*, **16**, 1449–1458.
13. Koczan, D., Guthke, R., Thiesen, H. J., et al. 2005, Gene expression profiling of peripheral blood mononuclear leukocytes from psoriasis patients identifies new immune regulatory molecules, *Eur. J. Dermatol.*, **15**, 251–257.
14. Proudfoot, N. J., Shander, M. H., Manley, J. L., Gefter, M. L. and Maniatis, T. 1980, Structure and in vitro transcription of human globin genes, *Science*, **209**, 1329–1336.
15. Shoyab, M., McDonald, V. L., Bradley, J. G. and Todaro, G. J. 1988, Amphiregulin: a bifunctional growth-modulating glycoprotein produced by the phorbol 12-myristate 13-acetate-treated human breast adenocarcinoma cell line MCF-7, *Proc. Natl. Acad. Sci. USA*, **85**, 6528–6532.
16. Mosavi, L. K., Cammett, T. J., Desrosiers, D. C. and Peng, Z. Y. 2004, The ankyrin repeat as molecular architecture for protein recognition, *Protein Sci.*, **13**, 1435–1448.
17. Subramaniam, S., Stansberg, C. and Cunningham, C. 2004, The interleukin 1 receptor family, *Dev. Comp. Immunol.*, **28**, 415–428.
18. Foell, D. and Roth, J. 2004, Proinflammatory S100 proteins in arthritis and autoimmune disease, *Arthritis Rheum.*, **50**, 3762–3771.
19. Lee, S. L., Tourtellotte, L. C., Wesselschmidt, R. L. and Milbrandt, J. 1995, Growth and differentiation proceeds normally in cells deficient in the immediate early gene NGFI-A, *J. Biol. Chem.*, **270**, 9971–9977.
20. Russell, L. and Forsdyke, D. R. 1991, A human putative lymphocyte G0/G1 switch gene containing a CpG-rich island encodes a small basic protein with the potential to be phosphorylated, *DNA Cell Biol.*, **10**, 581–591.
21. Kao, L. C., Germeyer, A., Tulac, S., et al. 2003, Expression profiling of endometrium from women with endometriosis reveals candidate genes for disease-based implantation failure and infertility, *Endocrinology*, **144**, 2870–2881.
22. Yoon, I. K., Kim, H. K., Kim, Y. K., et al. 2004, Exploration of replicative senescence-associated genes in human dermal fibroblasts by cDNA microarray technology, *Exp. Gerontol.*, **39**, 1369–1378.
23. Zandbergen, F., Mandard, S., Escher, P., et al. 2005, The G0/G1 switch gene 2 is a novel PPAR target gene, *Biochem. J.*, **392**, 313–324.

Journal of Autoimmunity 31 (2008) 79–89

Contents lists available at ScienceDirect

Journal of Autoimmunity

journal homepage: www.elsevier.com/locate/jautimm

MPO-ANCA induces IL-17 production by activated neutrophils *in vitro* via classical complement pathway-dependent manner

Akiyoshi Hoshino [a,b,c], Tomokazu Nagao [c,d], Noriko Nagi-Miura [e], Naohito Ohno [e], Masato Yasuhara [b], Kenji Yamamoto [a,b], Toshinori Nakayama [d], Kazuo Suzuki [c,d,*]

[a] International Clinical Research Center, Research Institute, International Medical Center of Japan, Tokyo, Japan
[b] Department of Pharmacokinetics and Pharmacodynamics, Hospital Pharmacy, Tokyo Medical and Dental University Graduate School, Tokyo, Japan
[c] Department of Bioactive Molecules, National Institute of Infectious Diseases, Tokyo, Japan
[d] Department of Immunology, Chiba University Graduate School of Medicine, Chiba, Japan
[e] Laboratory for Immunopharmacology of Microbial Products, School of Pharmacy, Tokyo University of Pharmacy and Life Science, Tokyo, Japan

ARTICLE INFO

Article history:
Received 8 February 2008
Received in revised form 23 March 2008
Accepted 30 March 2008

Keywords:
ANCA
Autoantibodies
Autoimmunity
β-Glucan
Candida albicans
Chemokine
Complement
Coronary arteritis
Crescentic glomerulonephritis
Cytokine
Fungal infection
Inflammation
IL-17A
IL-23
Mannoprotein
Myeloperoxidase
Neutrophils
Vasculitis

ABSTRACT

The elevation of serum anti-neutrophil cytoplasmic autoantibodies (ANCA) is significantly associated with the progression of some patients with systemic vasculitis. Especially, myeloperoxidase-specific ANCA (MPO-ANCA) play a pivotal role in the progression of systemic vasculitis including crescentic glomerulonephritis. Here we demonstrated that MPO-ANCA-activated neutrophils allow the local environment to differentiate Th_{17} cells through IL-6, IL-17A, and IL-23 production. We found a variety of elevated serum cytokines, especially IL-17A, in ANCA-mediated systemic vasculitis mice. Furthermore, activated peritoneal neutrophils *in vitro* also produced IL-17A and IL-23 in response to MPO-ANCA. Co-stimulation of fungal mannoprotein and complements significantly enhanced the MPO-ANCA-mediated *IL-17A* expression, but $F(ab')_2$ fragments of MPO-ANCA diminished the cytokine response. These results suggest that the activated neutrophils produce IL-17A and IL-23 in response to MPO-ANCA via classical complement pathway, which initiate the first steps of chronic autoimmune inflammation by allowing the local environment to develop Th_{17}-mediated autoimmunity.

1. Introduction

Neutrophils act as the initial innate immune response against invading microorganisms to produce reactive oxygen species by releasing their lysosomal peroxidases including myeloperoxidase (MPO), which is an essential molecule in the initiation and execution of the acute inflammatory response against microbial infection [1–5]. In particular, the MPO-specific anti-neutrophil cytoplasmic autoantibodies (MPO-ANCA, usually known as perinuclaear ANCA, p-ANCA) are significantly involved in the development of various kinds of vasculitis, including ANCA-associated rapid progressive glomerulonephritis (RPGN), and microscopic polyangiitis [6–9]. Previous studies have demonstrated that MPO is a major antigen for p-ANCA production by using MPO-deficient mice [10,11], and the adoptive transfer of MPO-reactive splenocytes into *Rag2*-deficient mice resulted in crescentic glomerulonephritis with a high MPO-ANCA titer [12]. The fact that high levels of MPO-ANCA resulted in

Abbreviations: Ab, antibody; ANCA, anti-neutrophil cytoplasmic antibody; CAWS, *C. albicans* water-soluble mannoprotein and β-glucan complex; GPCR, G-protein coupled receptor(s); H&E, hematoxylin/eosin; MPO, myeloperoxidase(s); MPO-ANCA, MPO-specific anti-neutrophil cytoplasmic autoantibody; PTX, pertussis toxin from *Bordetella pertussis*.

* Corresponding author at: Inflammation Program, Department of Immunology, Chiba University Graduate School of Medicine, Inohana 1-8-1, chuo-ku, Chiba 260-8670, Japan. Tel.: +81 43 221 8831; fax: +81 43 221 8832.
E-mail addresses: ksuzuki@faculty.chiba-u.jp, ksuzuki@nih.go.jp (K. Suzuki).

0896-8411/$ – see front matter © 2008 Elsevier Ltd. All rights reserved.
doi:10.1016/j.jaut.2008.03.006

kidney dysfunction is consistent with the observation that patients with ANCA-related RPGN showed significantly increased MPO activity and MPO-ANCA titer [13].

According to our established murine vasculitis model mice [14], activated neutrophils contribute to renal lesions as they do in the spontaneous crescentic glomerulonephritis-forming Kinjoh mouse (SCG/Kj mouse) [15,16]. The fact that the enhanced release of MPO from neutrophils was observed in the early phase of glomerulonephritis, indicates that activated neutrophils contribute to the development of active crescentic lesions in our model mice [14]. In addition, a significantly high level of IL-12p40 was observed [14]. Therefore, IL-23, which is a heterodimeric cytokine composed of the p40 subunit of IL-12 and a p19 subunit, has key roles in autoimmune diseases by driving the development of autoreactive IL-17-producing T lymphocyte (Th_{17}) cells [17]. IL-23 is also reported to activate the IL-17-mediated autoimmune pathway and promote chronic inflammation via cytokines IL-17, IL-6, and IL-8 by neutrophils and monocytes [18–20].

Several researchers have noted that MPO-ANCA are directly associated with the vascular endothelium [21]. It is assumed that higher titers of ANCA mediate neutrophil responses in vascular inflammation directly and indirectly [22]. Our findings that MPO-ANCA directly binds to the primary glomerular endothelium following upregulation of ICAM-1, VCAM-1, E-selectin, and promotion of TNF-α production [21], is consistent with the observation of Little et al. [23]. However, there is no information on how MPO-ANCA reacts to neutrophils to promote cytokine production.

This study clarified the relationship between the initial activation step of chronic autoimmune inflammation and systemic vasculitis. The results demonstrate that IL-6, IL-17, and IL-23 production by neutrophils in response to ANCA plays a significant role in the initiation of systemic inflammation.

2. Materials and methods

2.1. Mice and reagents

C57BL/6J mice were purchased from Japan Clea, Inc. (Tokyo, Japan) and maintained in the animal facility of the Research Institute, International Medical Center of Japan. All experiments were performed according to the Guidelines for Laboratory Animal Experiments in Research and with the approval of the both local ethics committees at the Research Institute, International Medical Center of Japan. Mouse complement fraction was purchased from Rockland Immunochemicals, Inc. (Gilbertsville, PA). MPO-ANCA (polyclonal anti-murine MPO Ab, collected from $MPO^{-/-}$ mice with MPO-immunization) and control IgG was prepared as described previously [14]. The $F(ab)'_2$ fragment of ANCA was prepared by (pierce). CAWS mannoprotein extracted from the culture supernatant of *C. albicans* (IFO 1385 strain) was prepared as previously described [24], and activation (121 °C, 2 atm for 30 min, by autoclave) was performed immediately before use. Magnetic nanoparticles ThermaMax® LSA(30) modified for cell isolation was kindly provided from Magnabeat Inc, Chisso Corp., Chiba, Japan [25].

2.2. ANCA-induced systemic vasculitis model

An ANCA-induced systemic vasculitis model was described previously [14]. In brief, C57BL/6J (male, 9 weeks old) mice were injected i.v. with 1 mg of MPO-ANCA after pretreatment with i.p. injection of CAWS (4 mg/mouse). On day 5, 1 mg of MPO-ANCA was injected i.v. 3 h after injection as secondary boost stimulation. After secondary stimulation, mice were observed and sacrificed when moribund or on day 10. For cytokine measurement experiments, two mice were sacrificed at the indicated time course (day 0.5, day1, day3, day5, day 5.25, day 5.5, day 6, day 7, day 8, and day10) in order to collect a series of sera and peritoneal lavage fluids. For histological analysis, kidneys and lungs were collected on day10. Tissue was immediately washed and fixed with 10% formaldehyde neutralized solution for 4 h, and the organs were embedded in paraffin, sliced to 4-μm thickness and affixed to a glass slide (Matsunami Glass Industries, Osaka, Japan) to perform hematoxylin/eosin (H&E), and periodic acid Schiff (PAS) staining.

2.3. Neutrophil extraction, in vitro culture and intracellular cytokine analysis

Murine peritoneal neutrophils were prepared as described previously [25]. In brief, peritoneal exudate cells acutely infiltrated in the peritoneal cavity of C57BL/6 mice 3 h after i.p. injection with 8% casein in PBS suspension solution were collected, and incubated with ThermaMax® conjugated with streptavidin (Magnabeat) pretreated with biotinylated anti-F4/80 Ab (Caltag Laboratories, Burlingame, CA) on ice for 30 min. Thereafter, the cells were incubated at 37 °C for 1 min, and the aggregated F4/80 cells with magnetic nanoparticles were removed under a magnetic field. The purified neutrophils were incubated with Hanks' balanced salt solution (HBSS) for 10 min, and plated on a pre-warmed culture dish. Neutrophils were cultured for 6 h in the presence of 25 ng/ml of Brefeldin A (Sigma–Aldrich, St. Louis, MO) and 1× monensin solution (BioLegend Inc, San Diego, CA) after being stimulated with ANCA or control IgG. Next, neutrophils were immediately stained with PE-conjugated anti-Gr-1 mAb (Pharmingen BD, San Diego, CA) and biotinylated anti-F4/80 mAb (Cedarlane, ON, Canada), and Streptavidin-PerCP-Cy5.5 (Pharmingen BD). Thereafter, the neutrophils were fixed and permeabilized with modified Cytofix/Cytoperm solution (Pharmingen BD) containing an adequate concentration of paraformaldehyde and saponin. Neutrophils were immediately stained with Alexa488-conjugated anti-IL-17A mAb (eBioscience, San Diego, CA), and analyzed by FACS Calibur (BD Biosciences). Images were acquired with a CCD camera DP-70 (Olympus, Japan) under fluorescent microscopy IX-81 (Olympus) equipped with a combination of adequate filter units.

2.4. Multiple cytokine and chemokine assay by Bio-Plex® and ELISA

Mouse serum (12 μl, undiluted) and peritoneal lavage fluids (12 μl, concentrated ×10) were used for the detection of 18 cytokines and chemokines in murine serum using the Bio-Plex® Cytokine Assay 18-Plex kit (BioRad Laboratories) according to the manufacturer's protocol, and analyzed by the Bio-Plex Luminex 100 XYP instrument for analysis. The cytokine concentrations were calculated using Bio-Plex Manager 3.0 software with a five-parameter curve-fitting algorithm applied for standard curve calculations. Murine IL-23(p19/p40) quantification in serum and culture media was measured with a murine IL-23(p19/p40) Ready-set-Go ELISA kit (eBioscience, San Diego, CA) according to the manufacturer's instructions.

2.5. Real-time quantitative RT-PCR of cytokine expression

Total cellular RNA from peritoneal neutrophils and splenocytes was isolated using RNeasy (QIAGEN, Valencia, CA). The total RNA was then reverse-transcribed into cDNA using the Superscript III RT kit (Invitrogen, Carlsbad, CA) and then it was amplified with specific oligonucleotide primers for IL-6, IL-12, IL-17A, and IL-23p19. The primer structures used in this experiment were as follows: IL-6 (sense 5′-TGG AGT CAC AGA AGG AGT GGC TAA-3′, antisense 5′-TCT GAC CAC AGT GAG GAA TGT CCA-3′); IL-12p35 (sense 5′-CCA AGG TCA GCG TTC CAA CA-3′, antisense 5′-AGA GGA GGT AGC GTG ATT GACA-3′); IL-12/IL-23 p40 (sense 5′-ACA GCA CCA GCT TCT TCA TCAG-3′, antisense 5′-TCT TCA AAG GCT TCA TCT GCAA-3′); IL-17A

(sense 5′-GCT CCA GAA GGC CCT CAGA-3′, antisense 5′-CTT TCC CTC CGC ATT GACA-3′), IL-23p19 (sense 5′-TGG CTG TGC CTA GGA GTA GCA-3′, antisense 5′-TTC ATC CTC TTC TTC TCT TAG TAG ATT CATA-3′); TGF-β1 (sense 5′-ATC CTG TCC AAA CTA AGG CTCG-3′, antisense 5′-ACC TCT TTA GCA TAG TAG TCC GC-3′); and GAPDH (sense 5′-AGT ATG ACT CCA CTC ACG GCAA-3′, antisense 5′-TCT CGC TCC TGG AAG ATG GT-3′). A real-time quantitative PCR analysis was performed using a SYBR® Green PCR Master Mix (Applied Biosystems, Foster City, CA) and the ABI 7700 sequence detector system (Applied Biosystems) by the following parameters: after an initiation incubation at 50 °C for 2 min and at 95 °C for 10 min, 40 cycles of denaturation at 95 °C for 15 s, annealing at 65 °C for 30 s, and extension at 72 °C for 45 s. The cytokine gene expression was compared to the expression of GAPDH by $2^{-\Delta(Ct)}$ and normalized by the expression under unstimulated conditions.

2.6. Statistical analysis

The data presented as the means ± 1 standard deviation (SD) were compared using the two-tailed Student's *t*-test and ANOVA (Fig. 5) with the KaleidaGraph 4.0 software program (Synergy Software, Reading, PA). *P*-values <0.05 were regarded as significant.

3. Results

3.1. ANCAs trigger the systemic vasculitis by promoting IL-6, IL-17, and IL-23 production from neutrophils

We previously established systemic vasculitis, including kidney glomeruli, lung and skin lesions, by co-administration of MPO-ANCA and CAWS (Fig. 1a) [14]. In this model, severe renal dysfunction such as proteinuria was observed after injection of CAWS and MPO-ANCA, respectively. However the severe onset of dysfunction occurred only after the co-administration of both. Initially, we investigated the combinatory effect of MPO-ANCA and CAWS on the onset of the systemic vasculitis. Neutrophil infiltration into kidneys is observed in both the ANCA-treated and ANCA plus CAWS-treated groups (Fig. 1b, left). On the other hand, neutrophil infiltration into the lung with interstitial hemorrhage was observed only after simultaneous injection of MPO-ANCA and CAWS (Fig. 1b, right). Pulmonary lesions with macrophage infiltration were also observed following CAWS dosage, indicating that alveolar macrophages are the principal effector immune cells in the lung lesions induced by CAWS exposure. These results suggest that simultaneous stimulation of MPO-ANCA and CAWS is required to activate neutrophils.

Since neutrophils produce IL-6 in response to MPO-ANCA mediated arteritis [26], we measured a series of serum cytokine levels to determine if they were correlated to neutrophil activation. The expression of 18 kinds of cytokines and chemokines were analyzed in mice that received MPO-ANCA injection and showed that IL-6, IL-17A, 12p40, and G-CSF were dramatically increased with the development of vascular lesions (see Fig. 2a). Notably, some chemokines were also significantly increased. However, the IL-12p70 level was quite low whereas a high titer of IL-12p40 was detected (Fig. 2a), prompting us to examine serum IL-23, which is a heterodimeric cytokine composed of the IL-12p40 and an IL-23p19 subunits. The serum IL-23 level increased just after MPO-ANCA injection, which is similar to the IL-6 profile (Fig. 2b), and then the IL-17A level was elevated. This data is consistent with the fact that IL-23 is a key regulator of IL-17A production [18,27].

To confirm the possibility that peritoneal neutrophils (the first cells to be exposed to MPO-ANCA) are the producers of IL-23, the cytokine level in peritoneal lavage fluid was evaluated. As expected, a higher level of IL-23 was produced in the peritoneal fluid (Fig. 2c). In addition to IL-6 production, IL-23 was also produced by peritoneal neutrophils on day 1. Consequently, IL-17A production was induced around day 5 (Fig. 2c). However, no IL-12p70 was observed in the peritoneal fluid (data not shown). To support this, the mRNA transcription level of *IL-23p19* in peritoneal exudate cells on day 1 and day 6 was also enhanced after MPO-ANCA co-stimulation (data not shown). The fact that *IL-17A* transcription was also induced around day 5, is consistent with the result of increased IL-17A levels in peritoneal lavage fluids. The *IL-17A* transcription in splenic $CD4^+$ T cells is elevated 10 days after MPO-ANCA exposure (Fig. 2d). In addition, *TGF-β1* mRNA transcription was also increased during induction of vasculitis. These results suggest that peritoneal resident neutrophils that react to MPO-ANCA in the peritoneal cavity are involved in triggering a massive systemic vasculitis by producing specific cytokines such as IL-6, IL-17A, and IL-23, following the activation of $CD4^+$ T cells that produce IL-17A.

3.2. Activated neutrophils have the ability to produce IL-17A in response to MPO-ANCAs

We confirmed the intracellular cytokine production of IL-17A in neutrophils to determine which cells in the peritoneal cavity produced IL-17A in response to MPO-ANCA. The peritoneal exudate cells include 55% of Gr-1^{hi}, $CD11b^{int}$, $F4/80^-$ acute inflammatory neutrophils, and 30% of Gr-1^{int}, $CD11b^{hi}$, $F4/80^+$ peritoneal macrophages (Fig. 3a). The potential IL-17A-productivity from $Gr1^+F4/80^-$ neutrophils was confirmed by PMA/ionomycin stimulation. Gr-1^{hi} neutrophils produced much more IL-17A in response to both MPO-ANCA and CAWS than Gr-1^{int} macrophages (Fig. 3b,c). These results suggest that Gr-1^{hi} neutrophils have the ability to produce IL-17A in response to autoantibodies specific to neutrophil components. To confirm this, we next measured the expression of cytokines and chemokines from peritoneal neutrophils using ELISA. Peritoneal neutrophils were purified by ThermaMax® LSA streptavidin-conjugated magnetic nanoparticles (Magnabeat Corp.), which acquired magnetism when they were aggregated by warming over 30 °C [25]. The nanoparticles bound to anti-F4/80 Abs ablated the Gr-1^{int}, $CD11b^{hi}$, $F4/80^+$ peritoneal macrophages (Fig. 4a). To test whether this separation process activates the neutrophils, we confirmed the surface expression of MPOs, whose expression is observed only on the membrane surface of activated neutrophils [28]. The surface expression of MPO is not observed in purified peritoneal neutrophils (Fig. 4b), indicating that the purification process of neutrophils with ThermaMax® nanobeads does not activate neutrophils [25]. Next we measured MPO-ANCA induced IL-17A and IL-23 production by purified peritoneal neutrophils *in vitro* (Fig. 4c). In addition, only co-stimulation of CAWS plus MPO-ANCA enhanced IL-6, IL-17A, and IL-23 production. No detectable cytokine expression was observed in response to IL-17A and IL-23 in splenic macrophages (data not shown), thus indicating that the responsiveness to MPO-ANCA is restricted to neutrophils. Surprisingly, the peritoneal neutrophils produced IL-6 in response to CAWS, which is consistent with the previous observation that neutrophils produce IL-6 in response to CAWS stimulation [26]. Peritoneal neutrophils produced much higher IL-6 in response to MPO-ANCA plus CAWS, whereas stimulation with only MPO-ANCA did not enhance IL-6 production. Control IgG affects less in IL-17A and IL-23 production (data not shown). These results suggest that MPO-ANCAs induce IL-17A and IL-23 production not by macrophages but by neutrophils. Therefore, the activated neutrophils have an ability to produce IL-17A in response to MPO-ANCA.

The peritoneal neutrophils produced detectable amounts of IL-6, IL-17A, and IL-23, and other cytokines (Table 1), indicating that the activated neutrophils mainly produce a series of chemokines instead of proinflammatory cytokines. In addition, a series of chemokines are produced by peritoneal neutrophils (Fig. 4d). The reactivity of the chemokines was classified into two groups: CAWS-sensitive

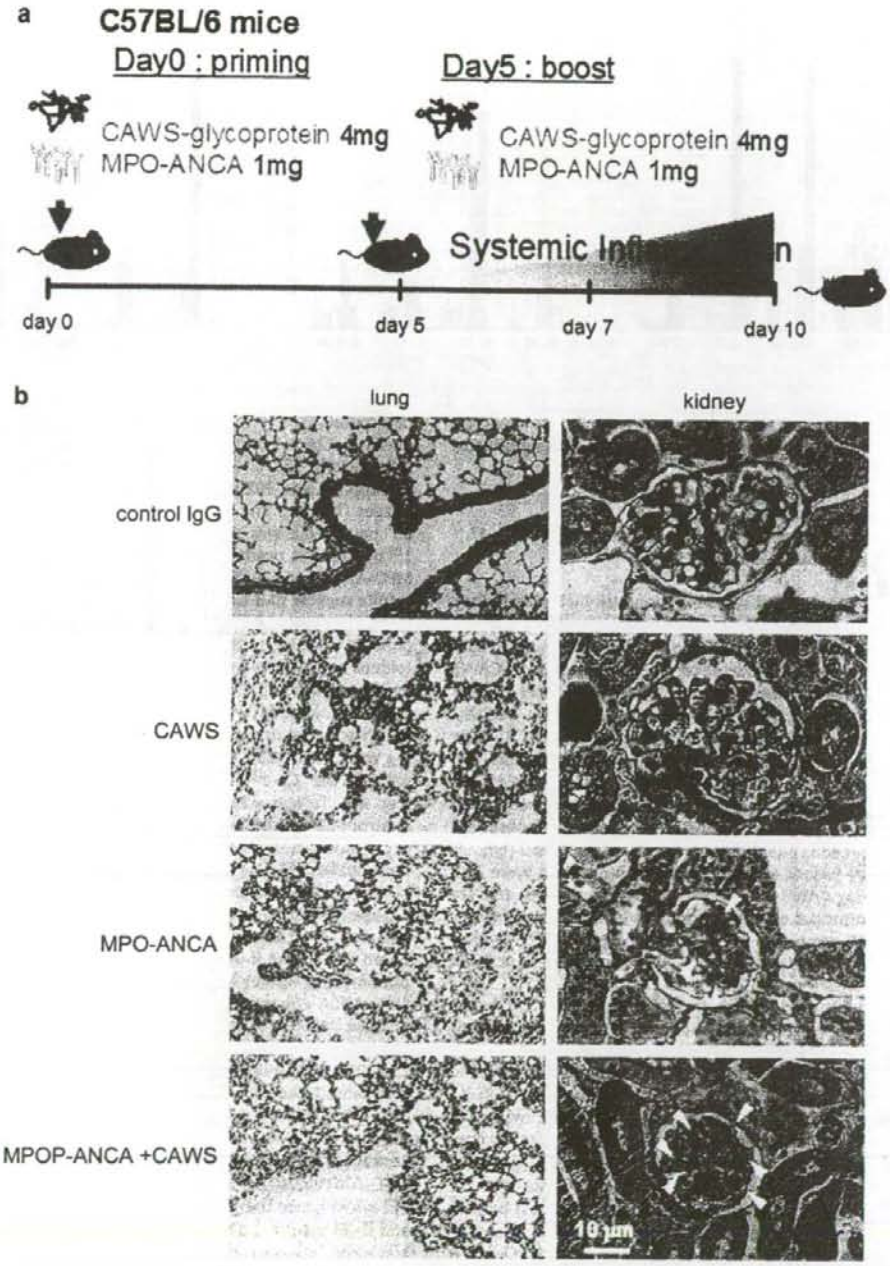

Fig. 1. ANCA induces massive systemic vasculitis in association with CAWS mannoprotein. (a) A schematic illustration of MPO-ANCA-induced murine experimental systemic vasculitis model. C57BL/6J mice (male, 9 weeks) were injected i.v. with MPO-ANCA (1 mg/mouse) after pretreatment with 4 mg of i.p. injection of CAWS mannoprotein. To develop the systemic vasculitis, MPO-ANCA (1 mg/mouse) was injected i.v. again on day 5. (b) A histopathological analysis of lung (HE stain, left) and kidney glomerulus (PAS stain, right) 7 days after induction of systemic vasculitis. The mice were treated with MPO-ANCA (1 mg ×2), control IgG(1 mg ×2), CAWS (4 mg/mouse ×2), and MPO-ANCA plus CAWS, respectively, according to the protocol shown in (a). A representative histology from 10 examinations is presented and similar histological findings were obtained in other examinations. Magnification ×200 (left) and ×1000 (right). The arrowheads indicate the infiltrated neutrophils in the glomeruli.